(amputation of Static Shapes and Voltages for Micromachined Deformable Mirrors with Nonlinear Electostatic Actuators

P.K C. Wang* *Senior Member, IEEE*, and F.Y. Hadaegh** *Senior Member, IEEE*

A bstract - **In modelling micromachined deformable mirrors with electrostatic actuators whose gap spacings arc of the same order of magnitude as that of the surface deformations, it is necessary to usc nonlinear models for the actuators. In this paper, wc consider micromachined deformable mirrors modelled by a membrane or plate equation with nonlinear electrostatic actuator characteristics. Numerical methods for computing the mirror deformation duc to given actuator voltages, and the actuator voltages required for producing the desired deformations at the actuator locations arc presented. The application of the proposed methods to circular deformable mirrors whose surfaces are modelled by elastic membranes is discussed in detail. Numerical results are obtained for a typical circular micromachined mirror with electrostatic act uators.**

1. Introduction

DEFORMABLE mirrors with electrostatic actuators have been widely used in various adaptive optical systems [I], [2] and spaceborne antennas **[3].** in 1977, Grosso and Yellin [4] developed a membrane mirror whose deformations were controlled by means of discrete electrostatic actuators. subsequently, various forms of deformable mirrors with electrostatic actuators have been developed [5]-[8]. The advent of silicon VLSI technology has made possible the integration of deformable mirrors with microelectronic circuitry. In 1983, Hornbeck [9] perfected a 51μm square deformable mirror with pixelated mirror elements. The mirror deformations were controlled by electrostatic actuators driven by microelectronic circuits which are integrated with the mirror assembly. his mirror was used primarily as a light modulator. Therefore it was unnecessary to control the mirror shape precisely. The present. work is motivated by the recent effort in exploiting micromachining technology to develop small deformable mirrors with pixelated electrostatic actuators for controlling the mirror shape precisely [10]-[1 3]. These mirrors have potential applications in adaptive optical systems for interferometers and large-aperture telescopes, and miniature imaging devices.

Previous analytical studies [I], [4] of large deformable mirrors with electrostatic actuators do not include the effect of mirror deformation on the actuator gap spacing. In micromachined deformable mirrors with electrostatic actuators, it is desirable to set the gap spacing as small as possible so as to minimize the operating voltage level. Consequently, the mirror surface deformations are of the same order of magnitude as that of the gap spacing. Thus, it is necessary to use nonlinear actuator models. Recently, Cai *et* al [14], and Gilbert *et al[15]* developed computational algorithms based on finite-cle,ncr,t method and iterative schemes which could be used for the numerical solution of nonlinear models of microelectron mechanical structures such as the deformable mirrors under consideration Here, wc make USC of the contraction mapping method for the determining the mirror deformation due to specified actuator voltages, and also propose a method for solving the inverse problem of determining the required actuator voltages to achieve a desired mirror deformation.

We begin with the development of mathematical models in the form of nonlinear partial differential equations describing the mirror surface deformations. "1'hell algorithms for computing the mirror deformation corresponding to specified actuator voltages, and for computing the required actuator voltages to produce a *given* set of mirror deformations at the actuator locations, are proposed. The application of these algorithms

* P.K.C. Wang is with the Department of Electrical Engineering, University of California, Los Angeles, CA 90024-1594.

** F Y Hadaegh is with the Jet Propulsion Laboratory, California Institute of Technology, Pasadena, CA 91109 -'8099.

to circular deformable mirrors whose surfaces arc modelled by elastic membranes is discussed in detail. The paper concludes with numerical results for a typical micromachined mirror with electrostatic actuators.

II. Mathematical Models for Deformable Mirrors

Figure 1 shows a sketch of a circular micromachined deformable-mirror formed by a thin elastic surface (eg. silicon nitride) coated with a thin electrically conducting film. The electrostatic actuators correspond to electrodes deposited on a ground plane over which the mirror is attached. A voltage is applied between an electrode and the mirror surface so that the actuator is responsible for pulling on a small portion of the surface. The desired mirror deformation is achieved by applying suitable voltages between the electrodes and the mirror surface. The fabrication of such mirrors is described *in* [11].

Let Ω be an open connected subset of the Euclidean plane R^2 with a piecewise smooth boundary $\partial\Omega$ representing the spatial domain of the mirror. For a rectangular mirror, Ω is specified by $\Omega_R = \{(x_1, x_2) \in R^2 : |x_1| < \ell_1, |x_2| < \ell_2\}$, where the $\ell_i's$ are specified lengths. For a circular mirror, Ω is specified by a disk $\Omega_C = \{(r, O), O \leq r < r_o, O \leq \theta \leq 2\pi\}$. Consider a mirror with P actuators. Each actuator electrode is specified by a patch Ω_j (a specified open connected subset of Ω), whose location is represented by $x_j = (x_{j1}, x_{j2})$ (an interior point Of Ω_j), $j = 1, \ldots P$. Figure 2 shows typical actuator electrode patches for rectangular and circular mirrors.

Assuming that the elastic surface deformation is in the linear regime, the downward displacement u(x) normal to the undeformed mirror surface at a point $x \in \Omega$ can be described by a partial differential equation of the form:

$$(Au)(x) = -f, \tag{1}$$

where f is the surface force density whose explicit form will be derived later, and $\mathcal{A}$ is a linear partial differential operator.

When the thickness-diameter ratio of the mirror surface is small (typically $<< 10^{-2}$) such that the bending energy is negligible compared to that duc to tensile stresses, the mirror surface may be regarded as an elastic membrane. Let σ_{ij} (x), $i, j = 1, 2$, denote the components of the symmetric stress tensor in the mirror surface at x satisfying the positivity condition

$$c_1 \| \xi \|^2 \leq \sum_{i=1}^{2} \sum_{j=1}^{2} \sigma_{ij}(x) \xi_i \xi_j \leq c_2 \| \xi \|^2 \tag{2}$$

for all $\xi = (\xi_1, \xi_2) \in R^2$ and $x \in \Omega$, where c_1 and c_2 arc known positive constants, and $\| . \|$ denotes the Euclidean norm. Then the operator A has the form:

$$(AU.)(X) = -\sum_{i=1}^{2} \sum_{j=1}^{2} \frac{\partial}{\partial x} \sigma_{ij}(x) \frac{\partial u}{\partial x_i}(x). \tag{3}$$

In the special case with uniform tension T, wc have $\sigma_{ij} = T\delta_{ij}$, where δ_{ij} denotes the Kronecker delta. Assuming that the mirror is clamped to its boundary $\partial\Omega$, u must satisfy the boundary condition:

$$u(x) = 0 \text{ for } x \in \partial\Omega. \tag{4}$$

When the thickness-diameter ratio of the mirror surface is large such that the bending energy is not negligible, one may model the mirror surface by a plate. For the case with uniform thickness h,

$$(Au)(x) = -D \left(\frac{\partial^4 u}{\partial x_1^4} + 2 \frac{\partial^4 u}{\partial x_1^2 \partial x_2^2} + \frac{\partial^4 u}{\partial x_2^4} \right)(x), \tag{5}$$

where D is the flexural rigidity of the mirror surface given try $Eh^3/\{12(1-\nu^2)\}$ with E being the Young's modulus, and ν the Poisson's ratio. Assuming clamped edge, the boundary conditions are given by

$$u(x) = O \text{ and } (\partial u/\partial n) = O \text{ at } \partial\Omega, \tag{5}$$

where $(\partial u/\partial \mathbf{n})$ denotes the outward normal derivative of u at $\partial\Omega$.

To derive an explicit expression for the surface force density f, we first consider the electrostatic force density over a patch Ω_j due to a specified static voltage V_j applied to the j-th actuator. Let do denote the distance between the undeformed flat mirror surface and the bottom plane. Under the assumption that the minimal width ρ_j of the patch Ω_j is large compared to d_o (typically, $\rho_j/d_o \geq 10$), the electrostatic force density duc to the j-th actuator can be described approximately by

$$f_e(\mathbf{x}) = \frac{\epsilon_o V_j^2}{2(d_o - u(\mathbf{x}))^2}\phi_j(x) \qquad \text{for all } x \in \Omega, \tag{7}$$

where ϵ_o is the permittivity of free space; and ϕ_j may be taken as the characteristic function of Ω_j (i.e., $\phi_j(\mathbf{x}) = 1$ if $x \in \Omega_j$; $\phi_j(\mathbf{x}) = 0$ if $x \in \Omega - \Omega_j$), or a weighting function which models the spatial variation of f_e duc to the fringing electric field near the boundary of $L?_j$. Assuming that the spatial variation of u over Ω_j is small, we may replace $u(\mathbf{x})$ by a weighted average of u over Ω_j defined by

$$\bar{u}_j = \omega_j^{-1}\int_{\Omega_j} w_j(\mathbf{x})u(\mathbf{x})d\Omega_j; \qquad \omega_j = \int_{\Omega_j} w_j(\mathbf{x})d\Omega_j, \tag{8}$$

where w_j is a suitable spatial weighting function. In the special case where $w_j(\mathbf{x}) = \delta(\mathbf{x} - \mathbf{x}_j)$ is the Dirac delta function, $\bar{u}_j$ reduces to $u(\mathbf{x}_j)$, where $u(\mathbf{x}_j)$ specifies the location of the j-th actuator.

Substituting the modified (7) into (1) leads to a nonlinear partial differential equation given by

$$(\mathcal{A}u)(\mathbf{x}) = -\sum_{j=1}^{P}\frac{\epsilon_o V_j^2}{2(d_o - u(\mathbf{x})^2)}\phi_j(\mathbf{x}) \tag{9}$$

defined on Ω, where $\mathcal{A}$ is defined by (3) for a membrane, and by (5) for a plate.

When the mirror deformations over Ω_j are small compared to d_o so that $do - \bar{u}_j \simeq do$, then (9) becomes linear. This approximation is poor when it, is applied to micromachined mirrors whose deformations arc of the same order of magnitude as that of *do*. Therefore we shall consider only the nonlinear model (9) in the subsequent development.

Let V denote the actuator voltage vector $(V_1, \ldots, V_P)^T$, and $V^2 = (V_1^2, \ldots, V_P^2)^T$, where $(\cdot)^T$ denotes transposition. Let $\mathbf{u} = (\bar{u}_1, \ldots, \bar{u}_P)^T$. The relation between u and V^2 can be expressed in the form

$$\mathrm{U(X)} = \sum_{j=1}^{P} p(\mathbf{x}, \bar{u}_j)V_j^2, \tag{lo}$$

where $p(\mathbf{x}, \bar{u}_j)$ corresponds to the mirror deformation at any point $x \in \Omega$ due to unit voltage applied to the j-th actuator with specified actuator gap $(d_o - \bar{u}_j)$. Explicit expressions for p can be found for special actuator electrode shapes by solving (9) directly by considering $\bar{u}_j$ as a known quantity. For an arbitrary actuator electrode shape, p can be expressed in terms of the Green's function $K = \mathrm{K(x, x')}$ associated with the boundary-value problem [16]:

$$(\mathrm{Au})(\mathbf{x}) = \delta(\mathbf{x} - \mathrm{X'}), \qquad \mathbf{x}, \mathbf{x}' \in \Omega, \tag{11}$$

with appropriate boundary conditions, where δ is the Dirac delta function, Here, the boundary-value problem for (9) can be reformulated as an integral equation for the mirror deformation u corresponding to given static actuator voltages Vj, $j = 1, \ldots P$:

$$u(\mathbf{x}) = \int_\Omega K(\mathbf{x}, \mathbf{x}')\sum_{j=1}^{P}\frac{\epsilon_o V_j^2}{2(d_o - \bar{u}_j)^2}\phi_j(\mathbf{x}')d\mathbf{x}' \triangleq \sum_{j=1}^{P} p(\mathbf{x}, \bar{u}_j)V_j^2, \tag{12}$$

where

$$p(\mathbf{x}, \bar{u}_j) = \frac{\epsilon_o}{2(d_o - \bar{u}_j)^2}\int_\Omega K(\mathbf{x}, \mathbf{x}')\phi_j(\mathbf{x}')d\mathbf{x}'. \tag{13}$$

Equation (12) is valid provided that $0 \leq u(x) < d_o$ for all $\mathbf{x} \in \Omega$.

Multiplying both sides of (12) by $w_j(\mathbf{x})$, and averaging the resulting equation over Ω_j lead to a set of 1' implicit nonlinear algebraic equations relating $\mathbf{u}$ and V^2. They can be written in the form

$$\mathbf{u} = \mathcal{N}_{V^2}(\mathbf{u}) \triangleq \mathbf{P}(\mathbf{u})\mathbf{V}^2, \tag{14}$$

where P'(u) is a P x P matrix whose (i,j)-th element corresponds to $\omega_i^{-1} \int_\Omega w_i(\mathbf{x}) p(\mathbf{x}, \tilde{u}_j) d\Omega_i$.

III. Computational Problems

We shall consider two basic computational problems associated with the deformable mirror. To simplify the subsequent development, only the case where $\tilde{u}_j = u(\mathbf{x}_j)$, j = 1,...1P, will be discussed.

A. *Mirror Deformation Corresponding to Specified Actuator Voltages*

Here, wc are given actuator voltages $V = (VI, ..., V_P)^T$. It is required to determine the corresponding mirror deformation $u = u(x)$, $x \in \Omega$. We observe from (12) that once the mirror deformation at all the actuator points are known, the solution to the boundary-value problem for (9) at *any* point in Ω can be determined *exactly*. l'bus, the computational problem can be decomposed into two basic steps:

Step (i): Determine the mirror displacement $\mathbf{u} = (u(\mathbf{x}_1), ... u(\mathbf{x}_P))^T$ at the actuator locations, This involves determining the fixed points of the mapping $\mathcal{N}_{V^2}$.

Step (ii): Substitute the $\mathbf{u}$ obtained from Step (i) into (12) and compute the mirror deformation $u = u(x)$ for any $x \in \Omega$.

in view of the form of (14), it is natural to use the contraction-mapping method [17] to determine u in Step (i). One may also usc other methods such as Newton's method for solving (14). However, the contraction-mapping algorithm has the simplest form, and it converges to a fixed point of $\mathcal{N}_{V^2}$ corresponding to a statically stable mirror deformation.

Let $\mathcal{U}$ be a closed bounded subset of the Euclidean space R^P, and $\mathbf{u}^0 \in$ U be an initial guess for the fixed point of $\mathcal{N}_{V^2}$. Then the iterative algorithm is given by

$$\mathbf{u}^{k+1} = \mathcal{N}_{V^2}(\mathbf{u}^k), \quad k = 0, 1, 2, \ldots \tag{15}$$

If $\mathcal{N}_{V^2}$ is a contraction mapping on $\mathcal{U}$ (i.e., there exists a constant $\alpha, 0 < \alpha < 1$ such that $\| \mathcal{N}_{V^2}(\mathbf{u}) - \mathcal{N}_{V^2}(\tilde{\mathbf{u}}) \| \leq \alpha \| \mathbf{u} - \mathbf{ii} \|$ for any u, $\tilde{\mathbf{u}} \in U$, *where* $\|\|$ denotes the Euclidean norm for R^P), then the sequence $\{\mathbf{u}^k, k = 0,1,2,. ..\}$ converges to a *unique* fixed point of $\mathcal{N}_{V^2}$ in U. Moreover, the sequence satisfies the estimate

$$\| \mathbf{U}^k - \mathbf{u}^{k'} \| \leq [\alpha^k/(1 - a)] \| \mathbf{u}^0 - \mathbf{u}^1 \|, \qquad k, k' = 0, 1, 2, \ldots. \tag{16}$$

To apply the contraction-mapping method to our problem, it is necessary to choose a suitable domain U for the mapping $\mathcal{N}_{V^2}$. This domain must be sufficiently small such that it contains only onc fixed point of $\mathcal{N}_{V^2}$. Here, we let $\mathcal{U} = \{\mathbf{u} \in R^P : 0 < u_i \leq \hat{d}, i = 1, ... P\}$, where d is a constant such that $O < d < do$. Next, wc shall derive a sufficient condition under which $\mathcal{N}_{V^2}$ maps $\mathcal{U}$ into $\mathcal{U}$ (i.e. $\mathcal{N}_{V^2}$ dots not map points in U to points outside U). Suppose that

$$M_{ij} \triangleq \int_\Omega K(\mathbf{x}_i, \mathbf{x}') \phi_j(\mathbf{x}') d\mathbf{x}' \geq 0 \text{ for } i, j = \text{I},. ..)\text{P}. \tag{1'7}$$

Then, from (12), wc have

$$0 \leq u(\mathbf{x}_i) = \sum_{j=1}^{P} \frac{\epsilon_o V_j^2 M_{ij}}{2(d_o - u(\mathbf{x}_j))^2} \leq \sum_{j=1}^{P} \frac{\epsilon_o V_j^2 \hat{M}}{2(d_o - u(\mathbf{x}_j))^2}, \tag{18}$$

where $\hat{M} = \max\{M_{ij}; i, j = 1, ... 1'\}$. Evidently, if

$$\epsilon_o \hat{M} \sum_{j=1}^{P} V_j^2 < 2(d_o - \hat{d})^2 \hat{d}, \tag{19}$$

then $\mathcal{N}_{V^2}$ maps $\mathcal{U}$ into 24. To derive a sufficient condition for $\mathcal{N}_{V^2}$ to be a contraction mapping on $\mathcal{U}$, consider

$$| p(x_i, u(x_j)) - p(x_i, \tilde{u}(x_j)) | \leq \frac{\epsilon_o f}{2} \int_\Omega K(x_i, x') \phi_j(x') dx' \frac{1}{(d_o - u(x_j))^2} - \frac{1}{(d_o - \tilde{u}(x_j))^2} . \tag{20}$$

Since the real-valued function f defined by $f(\zeta) = 1/(d_o - 02$ is strictly monotone increasing on the interval $[0, d_o[$, it follows from the mcar,-valu, theorem that

$$| f(\zeta) - f(\tilde{\zeta}) | \leq f'(\bar{\zeta}) | \zeta - \tilde{\zeta} | \leq f'(\hat{d}) | \zeta - \tilde{\zeta} | = \frac{2}{(d_o - \hat{d})^3} | \zeta - \tilde{\zeta} | \tag{21}$$

for all $\zeta, \tilde{\zeta} \in [0, \hat{d}[, \zeta \leq \bar{\zeta} \leq \tilde{\zeta}$, where $f' = df/d\zeta$. From (17), (19) and (21), we have

$$| p(x_i, u(x_j)) - p(x_i, \tilde{u}(x_j)) | \leq \frac{\epsilon_o M_{ij}}{(d_o - \hat{d})^3} | u(x_j) - \tilde{u}(x_j) | \tag{22}$$

Using (14),(22), and the Schwarz inequality [17], we obtain the estimate

$$\| \mathcal{N}_{V^2}(\mathbf{u}) - \mathcal{N}_{V^2}(\tilde{\mathbf{u}}) \| \leq \left[\sum_{i=1}^{P} \left(\sum_{j=1}^{P} | p(x_i, u(x_j)) - p(x_i, \tilde{u}(x_j)) | V_j^2 \right)^2 \right]^{1/2}$$

$$\leq \left[\sum_{i=1}^{P} \left(\sum_{j=1}^{P} \frac{\epsilon_o M_{ij}}{(d_o - \hat{d})^3} | u(x_j) - \tilde{u}(x_j) | V_j^2 \right) \right]^{1/2}$$

$$\leq \frac{\epsilon_o \hat{M} \sqrt{P}}{(d_o - \hat{d})^3} \left(\sum_{j=1}^{P} | u(x_j) |^2 \right)^{1/2} \left(\sum_{j=1}^{P} V_j^4 \right)^{1/2}$$

$$= \frac{\epsilon_o \hat{M} \sqrt{P}}{(d_o - \hat{d})^3} \| \mathbf{u} - \tilde{\mathbf{u}} \| \| \mathbf{V}^2 \| \tag{23}$$

'1'bus, under condition (19) and

$$0 < \alpha \triangleq \frac{\epsilon_o \hat{M} \sqrt{P}}{(d_o - \hat{d})^3} \| \mathbf{V}^2 \| < 1, \tag{24}$$

$\mathcal{N}_{V^2}$ is a contraction mapping on $\mathcal{U}$. Conditions (19) aud (24) are conservative since they are independent of the sizes of the spatial domains of the actuators. Sharper sufficient conditions for contraction can be derived for specific actuator electrode patterns. We observe that, for a nonzero $\| \mathbf{V}^2 \|$, the constant α defined in (24) tends to infinity as $\hat{d} \to d_o$. '1'bus, in order to satisfy $\alpha < 1$, $\| \mathbf{V}^2 \|$ must be reduced accordingly as d increases towards d_o. This situation can be explained by considering the simplest case with one actuator located at xl. In this case, (14) reduces to a single algebraic equation in the following normalized form:

$$\tilde{u}_1/d_o = \mathcal{N}_{V^2}(\tilde{u}_1) \triangleq \kappa V_1^2/(1 - \tilde{u}_1/d_o)^2, \tag{14'}$$

where $\tilde{u}_1 = u(x_1)$, and κ is a positive constant given by

$$\kappa = \frac{\epsilon_o}{2 d_o^3} \int_{\Omega_1} K(x_1, x') \phi_1(x') dx' \tag{14"}$$

Figure 3 shows the graphs of $\mathcal{N}_V$ for various values of $\kappa V_1^2 > 0$. Their intersections with the diagonal line give the normalized fixed points of $\mathcal{N}_{V_1^2}$. Evidently, for sufficiently small κV_1^2 (Case *(a))*, $\mathcal{N}_{V_1^2}$ has two fixed

points, implying the existence of two solutions to (9). The larger fixed point is unstable. When κV_1^2 equals the critical value 4/27, these two fixed points merge into one as depicted by Case (b). If κV_1^2 is further increased, $\mathcal{N}_{V_1^2}$ no longer has a fixed point, implying the nonexistence of a solution to (9). The critical value of κV_1^2 in Case (b) corresponds a bifurcation point at which buckling occurs [25]. Note that for Case (a), in order for $\mathcal{U} = [0, \hat{d}]$ to be a domain of contraction for $\mathcal{N}_{V_1^2}$, d must be less than the unstable fixed point which tends to d_o as $\kappa V_1^2 \to +\infty$. This conclusion is also exhibited by the form of the contraction constant α given in (24).

Now, having computed the mirror deformation $u = u(x)$ for $x \in \Omega$ corresponding to given actuator voltages V_j, $j = 1, \ldots, P$, one may proceed to express u in terms of orthogonal polynomials such as Legendre or Zernike polynomials. The coefficients of the polynomial can be computed from the given values of u over a finite set of points in Ω using standard methods [], [22].

B. *Actuator Voltages Corresponding to Specified Mirror Deformations at the Actuator Locations*

Now, we consider the inverse problem of computing the actuator voltages which produce a specified u corresponding to the desired mirror displacements at the specified locations X3, . . . x_Q in Ω. Here, the points x_j need not correspond to the actuator locations. When the desired mirror deformation at specified locations XI, . . . , x_Q in Ω. Here, the points x_j, $j = 1, \ldots, Q$, need not correspond to the actuator locations. When the desired mirror deformation $u_d = u_d(x)$ is expressed in terms of a set of coefficients associated with a specified basis $\{\varphi_i = \varphi_i(x), i = 1)2, \ldots\}$ (i.e., $u_d(x) = \sum_i \alpha_i \varphi_i(x)$), *we* define the desired mirror displacement vector $\mathbf{u}_d$ by

$$\mathbf{u}_d = \left(\sum_i \alpha_i \varphi_i(x_1), \ldots, \sum_i \alpha_i \varphi_i(x_Q) \right)^T. \tag{25}$$

It follows from (10) that $\mathbf{u}_d = \tilde{\mathbf{P}}(\mathbf{u}_d)\mathbf{V}^2$, where $\tilde{\mathbf{P}}(\mathbf{u}_d)$ is a linear transformation on R^P into R^Q represented by a $Q \times P$ matrix whose i-th row is $(p(\hat{x}_i, u_d(x_1)), \ldots, p(\hat{x}_i, u_d(x_P)))$. When $Q = P$, and $\hat{x}_i$ corresponds to the location of the i-th actuator, $\tilde{\mathbf{P}}(\mathbf{u}_d)$ reduces to $\mathbf{P}(\mathbf{u}_d)$ as defined in 14). Now, the required actuator voltages may be obtained by

$$\mathbf{V}^2 = \tilde{\mathbf{P}}^+(\mathbf{u}_d)\mathbf{u}_d, \tag{26}$$

where $\tilde{\mathbf{P}}^+(\mathbf{u}_d)$ is the pseudoinverse [18] of $\mathbf{P}(\mathbf{u}_d)$, and $\mathbf{V}^2$ corresponds to the vector in R^P which minimizes $\| \mathbf{u}_d - \tilde{\mathbf{P}}(\mathbf{u}_d)\mathbf{V}^2 \|$. In the special case where $\mathbf{P}(\mathbf{u}_d)$ is nonsingular, $\tilde{\mathbf{P}}^+(\mathbf{u}_d)$ reduces to the usual inverse of $\tilde{\mathbf{P}}(\mathbf{u}_d)$. In general, it is possible that some components of $\mathbf{V}^2$ obtained from (26) are negative. This implies that the desired mirror displacement $\mathbf{u}_d$ is not attainable by the downward electrostatic forces produced by the actuators, A trivial example of an unattainable desired mirror surface is one with a concave shape. An alternate formulation to this problem is to find an element w^* in the closed bounded convex set $V = \{\mathbf{w} \in R^P : \mathbf{w} \geq \mathbf{0}$ **and** $\| \mathbf{w} \| \leq \bar{V}^2\}$ **such** that

$$J(\mathbf{w}^*) \leq J(\mathbf{w}) \text{ for all } w \in V, \tag{27}$$

where $J(\mathbf{w}) = \| \mathbf{u}_d - \tilde{\mathbf{P}}(\mathbf{u}_d)\mathbf{w} \|^2$, and $\bar{V}^2$ is a sufficiently small positive number. This is a convex programming problem. Its numerical solution can be obtained using the extended gradient-projection method [1 9].

IV. Circular Deformable-Mirror

Consider a circular deformable mirror with normalized spatial domain given by the unit disk $\tilde{\Omega}_C = \{(\tilde{r}, \theta): 0 \leq \tilde{r} < 1, 0 < \theta \leq 2\pi\}$, where $\tilde{r} = r/r_o$, and r_o is the mirror radius. Let $\tilde{\Omega}_j$ denote the normalized effective actuator spatial domain Ω_j. For specificness, we shall use a membrane model for the mirror surface deformations. Assuming that the mirror surface has uniform thickness and tension T, the partial differential equation corresponding to (3) arid (8) in cylindrical coordinates is given by

$$\frac{\partial^2 u}{\partial \tilde{r}^2} + \frac{1}{\tilde{r}} \frac{\partial u}{\partial \tilde{r}} + \frac{1}{\tilde{r}^2} \frac{\partial^2 u}{\partial \theta^2} = - \sum_{j=1}^{P} \frac{\epsilon_o}{2T} \left(\frac{r_o V_j}{d_o - u(\tilde{x}_j)} \right)^2 \tilde{\phi}_j(\tilde{x}_j) \tag{28}$$

with boundary condition:

$$u(\tilde{\mathbf{x}}) = 0 \qquad \text{for all } \mathrm{x} = (\tilde{r}, \theta) \in \partial\tilde{\Omega}_C, \tag{29}$$

where $\tilde{\mathbf{x}}_j = (\tilde{r}_j, \theta_j)$, and $\tilde{\phi}_j$ denotes the characteristic function of $\tilde{\Omega}_j$.

Using the explicit expression for the solution of the elliptic partial differential equation (1) with boundary condition (29) and arbitrary right-hand-side f [20], [21], (28) and (29) can be reformulated as a nonlinear integral equation of the form

$$u(\tilde{r}, \theta) = \frac{r_o^2}{2\pi T} \int_0^{2\pi} \int_0^1 K(\tilde{r}, \theta, \rho, \xi) f(\rho, \xi, u) \rho d\rho d\xi, \tag{30}$$

where $K = K_1 + K_2$, and

$$K_1(\tilde{r}, \theta, \rho, \xi) = -\left(\ln(\tilde{r}) + \sum_{n=1}^{\infty} \frac{\rho^n}{n} (\tilde{r}^n - \tilde{r}^{-n}) \cos(n(\xi - \theta))\right) \{U(\rho) - U(\rho - \tilde{r})\}, \tag{31}$$

$$K_2(\tilde{r}, \theta, \rho, \xi) = -\left(\ln(\rho) + \sum_{n=1}^{\infty} \frac{\tilde{r}^n}{n} (\rho^n - \rho^{-n}) \cos(n(\xi - \theta))\right) \{U(\rho - \tilde{r}) - U(\rho - 1)\}, \tag{32}$$

$$f(\rho, \xi, u) = \sum_{j=1}^{P} \frac{\epsilon_o}{2} \left(\frac{V_j}{d_o - u(\tilde{\mathbf{x}}_j)}\right)^2 \tilde{\phi}_j(\rho, \xi), \tag{33}$$

where U denotes the unit-step function. It is shown in Appendix A that

$$\left| \int_0^{2\pi} \int_0^1 K(\tilde{r}, \theta, \rho, \xi) \phi_j(\rho, \xi) \rho d\rho d\xi \right| \leq \hat{M} = \pi(\exp(-7/3) - 2\ln(3/5) + 21/10) \text{ for all } (\tilde{r}, \theta) \in \tilde{\Omega}_C \tag{34}$$

Applying conditions (19) and (24) to this case, a sufficient condition for $\mathcal{N}_{\mathbf{V}^2}$ to be a contraction mapping on $\mathcal{U}$ (defined in Sec.]]) is that

$$\frac{r_o^2 \epsilon_o}{2T} \| \mathbf{V} \|^2 (\exp(-7/3) - 2\ln(3/5) + 21/10) \leq 2(d_o - \hat{d})^2 \hat{d}, \tag{35}$$

and

$$r_o^2 \epsilon_o (\exp(-7/3) - 2\ln(3/5) + 21/10) \frac{\sqrt{P} \| \mathbf{V}^2 \|}{2T(d_o - \hat{d})^3} < 1. \tag{36}$$

The bound in (35) has a maximum at $\mathrm{d} = d_o/3$, which is about the onset of the well-known pull-in instability in structures of this type. 'J'bus, for a $\mathrm{d} < d_o/3$, and any given any $\mathbf{V}$ satisfying (35) and (36), the corresponding mirror deformation can be computed iteratively using the algorithm given by (1 5).

Now, we consider the problem of determining the actuator voltages $\mathbf{V}$ corresponding to specified desired static mirror deformations at the actuator locations. Here, the desired mirror deformation $u_d = u_d(\mathbf{x})$ is expressed in terms of Zernike polynomials [22] ,[23]:

$$u_d(\tilde{r}, \theta) = \sum_{j=1}^{\infty} \alpha_j Z_j(\tilde{r}, \theta), \tag{37}$$

where $\alpha_j's$ arc specified real coefficients, ancl

$$Z_j = \begin{cases} \sqrt{n+1} R_n^m(\tilde{r}) \sqrt{2/\pi} \cos(m\theta) & \text{for } j \text{ even and } m \neq 0, \\ \sqrt{n+1} R_n^m(\tilde{r}) \sqrt{2/\pi} \sin(m\theta) & \text{for } j \text{ odd and } m \neq 0, \\ \sqrt{n+1} R_n^0(\tilde{r}) / \sqrt{\pi} & \text{for } m = 0 \end{cases} \tag{38}$$

The functions R_n^m arc radial polynomials defined by

$$R_n^m(\tilde{r}) = \sum_{s=0}^{(n-m)/2} (-1)^s \frac{(n-s)!}{s!\left(\frac{n+m}{2}-s\right)!\left(\frac{n-m}{2}-s\right)!}\tilde{r}^{n-2s} \tag{39}$$

The degree of the polynomial n and the azimuthal frequency m arc positive integers satisfying $m \leq n$ and $n - m$ even. The radial polynomials R_n^m are normalized such that $R_n^m(1) = 1$. The index j is a mode ordering number which may be defined in many ways. Here, wc adopt Nell's convention [23] where the numbering sequence of the index j of Z_j proceeds as follows: for a given n, modes with a lower m are arranged first. When $m = n$, the even j terms correspond to the symmetric modes defined by $\cos(m\theta)$, while the odd j terms correspond to the antisymmetric modes defined by $\sin(m\theta)$.

Evaluating u_d given by (37) at the actuator locations $\tilde{\mathbf{x}}_j = (\tilde{r}_j, \theta_j)$ gives

$$\mathbf{u}_d = \left(\sum_{i=1}^{\infty} \alpha_i Z_i(\tilde{r}_1, \theta_1), \ldots \sum_{i=1}^{\infty} \alpha_i Z_i(\tilde{r}_P, \theta_P)^T\right). \tag{40}$$

The i-th row of the matrix $\mathbf{P}(\mathbf{u}_d)$ is given by

$$\mathbf{p}(\tilde{\mathbf{x}}_i, \mathbf{u}_d) = \left(\frac{r_o^2 \epsilon_o}{2(d_o - u_d(\tilde{\mathbf{x}}_1))^2} \int_{\tilde{\Omega}_C} K(\tilde{\mathbf{x}}_i, \tilde{\mathbf{x}}')d\tilde{\mathbf{x}}', \ldots, \frac{r_o^2 \epsilon}{2(d_o - u_d(\tilde{\mathbf{x}}_P))^2} \int_{\tilde{\Omega}_C} K(\tilde{\mathbf{x}}_i, \tilde{\mathbf{x}}')d\tilde{\mathbf{x}}'\right), \tag{41}$$

thus, given $\mathbf{u}_d$, the corresponding $\mathbf{V}^2$ can be determined from (26).

V. Numerical Examples

Now, wc apply the results in Sections IV and V to a typical circular micromachined silicon mirror with radius $r_o = 0.5$ cm and tension $T = 100 N/m$. The actuators consist of a center pad with radius $r_i = 0.2$ cm, and eight fan-shaped actuators. The fan-shaped actuators are centered along circles with radii 0.3 and 0.4 cm and with angles separated by $\pi/2$ radians. Moreover, they have uniform radial width of 0.09 cm land angular aperture of $0.95\pi/2$ radians. The sum of the characteristic functions of the actuator spatial domains is shown in Fig.4. The distance d_o between the undeformed flat mirror surface and the bottom plane is set at $10\mu m$. Explicit expressions for the elements of the matrix $\mathbf{P}(\mathbf{u})$ defined in (14) for fan-shaped and center pad actuators are given in Appendix]].

First, we apply the contraction mapping algorithm (15) to compute the mirror deformation corresponding to given actuator voltages $\mathbf{V}$. For the foregoing parameter values, conditions (35) and (36) for $\mathcal{N}_{\mathbf{V}^2}$ to be a contraction mapping are given explicitly by

$$\| \mathbf{V} \|^2 \leq 0.56144\hat{d}(10 - \hat{d})^2, \qquad \| \mathbf{V}^2 \| < 0.09357(10 - \hat{d})^3, \tag{42}$$

where $\hat{d}$ is given in microns, Evidently, for this case, (42) represents a conservative condition. This is due to the fact that the size of the actuator spatial domains is not taken into account in the derivation of (35) and (36). Actual computational experience revealed that convergence of algorithm (15) is attainable for much larger values of $\| \mathbf{V} \|$. Figure 5 shows a typical actuator voltage pattern corresponding to $\mathbf{V} = (5,10,5,\ 35,10,10,5,35,10)7'$ volts which does not satisfy (42). The norm of the difference of the mirror deformation u between two successive iterations as a function of iteration number is shown in Fig.6. The initial guess for the mirror deformation is given by $u(\tilde{r}, \theta) = (1 - \tilde{r}^2)$ pm. Figure 7a shows the computed mirror deformation. The radial profiles at $\theta = -\pi/4$ and $\pi/2$ radians, and the level curves of the computed mirror deformation are shown in Figure 7b and 7c respectively. Next, we reduce the actuator gap do to 6 microns while maintaining the same V, Figure 8 shows the norm of the difference of the mirror deformation u between two successive iterations as a function of iteration number starting with the flat mirror as the initial guess. here, we observe an oscillatory behavior of the iterated solution sequence indicating that the initial guess is outside the domain of contraction,

Now, let the desired mirror deformation u_d be specified by Zernike coefficients $\alpha_1 = 2.45\sqrt{\pi}\mu m, \alpha_4 = -1.4435\sqrt{\pi}\mu m$, and $\alpha_{11} = 0.0225\sqrt{\pi}\mu m$. Thus

$$u_d(\tilde{r}, O) = (2.45 Z_1(\tilde{r}) - 1.4435X4(F) + 0.0225 Z_{11}(\tilde{r}))\sqrt{\pi}$$

$$= (2.45 - 1.4435\sqrt{3}(2\tilde{r}^2 - 1) + 0.0225\sqrt{5}(6\tilde{r}^4 - 6\tilde{r}^2 + 1)) \text{ pm.} \quad (43)$$

The above u_d satisfies the boundary condition $u_d(1, \theta) = O$. Figure 9 shows the level curves and surface of the desired mirror deformation. Evaluating u_d at the center-pad radial point $r_1/2 = 0.1$ cm, and at the remaining actuator locations gives $\mathbf{u} = (8.488, 5.549, 3.068, 5.549, 3.068, 5.549, 3.068, 5.549, 3.068)^T \mu$m. The corresponding P(u) is given by

$$\mathbf{P(u)} = \begin{vmatrix} 0.5002 & 0.0053 & 0.0013 & 0.0092 & 0.0022 & 0.0092 & 0.0022 & 0.0053 & 0.0013 \\ 0.1979 & 0.0183 & 0.0047 & 0.0036 & 0.0009 & 0.0019 & 0.0005 & 0.0036 & 0.0009 \\ 0.0864 & 0.0087 & 0.0052 & 0.0017 & 0.0004 & 0.0008 & 0.0002 & 0.0017 & 0.0004 \\ 0.1979 & 0.0036 & 0.0009 & 0.0183 & 0.0047 & 0.0036 & 0.0009 & 0.0019 & 0.0005 \\ 0.0864 & 0.0017 & 0.0004 & 0.0087 & 0.0052 & 0.0017 & 0.0004 & 0.0008 & 0.0002 \\ 0.1979 & 0.0019 & 0.0005 & 0.0036 & 0.0009 & 0.0183 & 0.0047 & 0.0036 & 0.0009 \\ 0.0864 & 0.0008 & 0.0002 & 0.0017 & 0.0004 & 0.0087 & 0.0052 & 0.0017 & 0.0004 \\ 0.1979 & 0.0036 & 0.0009 & 0.0019 & 0.0005 & 0.0036 & 0.0009 & 0.0183 & 0.0047 \\ 0.0864 & 0.0017 & 0.0004 & 0.0008 & 0.0002 & 0.0017 & 0.0004 & 0.0087 & 0.0052 \end{vmatrix} \times 10^{-7} \quad (44)$$

which is nonsingular. The corresponding actuator voltages which produce the desired **u** are given by $V^2 = P(u)^{-1}u$ or $V = (9.6254, 0.1328, 41.7857, 30.1328, 41.7857, 30.1328, 1.7857, 30.1328, 41.7857)^T$ **volts.** Figure **10a shows the actual and desired mirror deformations** along **a radial** line at an angle of $\pi/4$ radians. Their difference is shown in Fig.10b. It can be seen that the actual mirror deformations at the actuator radial points 0.1,0.3, and 0.4 cm match exactly with the desired values as expected. The level curves and surface of the deformed mirror corresponding to the computed V are shown in Fig.11.

VI. Concluding Remarks

Recently, precision micromachined silicon mirrors with electrostatic actuators were successfully fabricated and tested at the Jet Propulsion Laboratory [] 1]. The experimental results were in close agreement with the computational results using the membrane models with nonlinear actuator characteristics described here. The details will be reported in the near future [24].

in contrast with finite-element methods which involve spatial discretization resulting in a large number of nonlinear algebraic equations to be solved, the computational methods presented here do not require such discretization. Once the mirror deformations at the actuator locations corresponding to given actuator voltages are computed, the mirror deformation at any point can be computed as accurately as desired. Moreover, the number of nonlinear algebraic equations to be solved is equal to the number of actuator electrodes. Finally, the methods presented here may also be applicable to large deformable mirrors with actuator forces which are describable by nonlinear algebraic functions of the local mirror deformations.

Acknowledgments

The authors wish to acknowledge many helpful discussions with M. T,. Agronin, R.K. Bartman, L.M. Miller, arid R.L. Norton on micromachined-mirror model validation. Thanks arc also due to the referees for their helpful comments and suggestions. This work was performed at the Jet, Propulsion Laboratory, California institute of2'ethnology, rrndcr contract with the National Aeronautics and Spacc Administration n. The work of P.K.C. Wang was also supported by NSF Grant ECS 92-13301.

References

[1] R.K. Tyson, *Principles of Adaptive* Optics, New York: Academic Press, 1991.

[2] M .A. Ealey, "Active and adaptive optical components: the technology and future trends," *Adaptive Optics and Optical Structures*, R. K. Tyson, J. Schulte in den Bäumen, Editors, *Proc. SPIE*, vol. 1271, pp.2-34, 1991.

[3] J ,11. Lang and D.H. Staelin, "Electrostatically figured reflecting membrane antennas for satellites," *IEEE Trans. Automat. Contr.*, vol.27, pp.666-670, *1982*.

[4] R.P. Grosso and M. Yellin, "The membrane mirror as an adaptive optical element," *J. Opt. Sot. Am.* vol. **67,** pp.399-406, **1967.**

[5] W.G. Thorburn **and L. Kaplan, "A low voltage** electro-distortive **mirror** system **for** wavefront **control,"** *Active and Adaptive Optical Components*, M.A. Ealey, Editor, *Proc. SPIE*, vol. *1543,* pp.52-63, *1991.*

[6] M .A. Ealey, "Precision electrodisplacive micro-actuators," *Precision Engineering and Opto-mechanics, I).* Vukobratovich, Editor, *Proc. SPIE*, vol.1167, pp.85- *102, 1989.*

[7] M.A. Ealey, and J l'. Washeba, "Continuous facesheet low voltage deformable mirrors," *Opt. Engr.* vol. 29, pp.1191-1198, 1990.

[8] M.A, Ealey and C.E. Wheeler, "Integrated wavefront corrector," *Adaptive Optics and Optical Structures,* R.K. Tyson, J. Schulte in den Bäumen, Editors, *Proc. SPIE*, vol. 1271, pp.254-264, 1990.

[9] L.J. Hornbeck, " 128 x 128 deformable mirror device," *IEEE Trans. Electron Devices,* vol. *ED* - 30, pp.539-545, *1983.*

[10] M.],. Agronin, R.K. Bartman, F.Y. Hadaegh, W. Kaiser, aud P.K.C. Wang, "Control of mi cromachined deformable mirrors," *Proc. NASA/JPL Workshop* 071 *Micro-technologies and Applications to Space Systems,* May, *1992,* Pasadena, CA., JPL Publication 93-8, pp.225-246, 1993.

[11] L.M. Miller *et* aL,''l'abrication and characterization of a micromachined deformable mirror for adaptive optics," *Space Astronomical Telescopes and Instruments, Proc. SPIE*, April, 1993.

[12] M. Hisanaga, '1'. Koumura, and T. Hattori, "lubrication of 3-dimensionally shaped Si Diaphragm dynamic focusing, mirror," *Proc. IEEE MEMS Workshop, pp.30-35, 1993.*

[13] G. Vdovin and S. Middelhoek, " Deformable mirror display with continuous reflecting surface micromachined in silicon," *Proc. IEEE MEMS Workshop,* pp.61-65, *1995.*

[14] X. Cai *et al,* "A relaxation/~ nultipole-accelerated scheme for self-consistent electromechanical analysis of complex 3--1) microelectro-mech anical structures, " *Proc. IEEE/A CM Int. Conf. Computer-Aided Design,* Santa Clara, California, pp.283-86, 1993,

[15] J .R. Gilbert, R. Legtenberg, and S.D. Senturia, " *3D* coupled electro-mechanics for MEMS: applications of CoSolve-*EM ," Proc. IEEE MEMS Workshop,* pp.1 *22-127,* 1995.

[16] I. Stakgold, *Boundary Value Problems of Mathematical Physics,* vol.1, *New* York: MacMillan, 1967.

[17] A.N. Kolmogorov and S.V. Fomin, *Elements of the Theory of Functions and Functional Analysis,* vol 1, *New* York: Graylock Press, 1957.

[18] R. Penrose, **"A** generalized inverse for matrices, " *Proc. Cambridge Phil. Sot.* vol.51, part 3, pp.406-413, 1955.

[]9] D.G. Luenberger, *Introduction to Linear and Nonlinear Programming,* Reading: Addisor,-Wesley, 1965.

[20] P.M. Morse and H. Feshbach, *Methods of Theoretical Physics,* vol.II, *New* York: McGraw-Hill, 1953.

[21] E.S. Claflin and N. Bareket, "Configuring an electrostatic membrane mirror by least-squares fitting with analytically derived influence functions, " *J. Opt. Soc. Am.*, vol. A3, p.1 833-1839, 1986.

[22] M. horn and E. Wolf, *Principles of Optics,* 6-th Edition (with corrections), Oxford: Pergamon Press, 1986.

[23] R.J. Nell, " Zernike polynomials and atmosphere turbulence," *J. Opt. Soc. Am.* vol. 66, pp.207-211, 1976.

[24] R.C. Gutierrez, R.K. Bartman, L.M. Miller, and P.K.C. Wang, " Experimental validation of membrane model for micromachined deformable mirrors with electrostatic actuators," (in preparation).

[25] P.K.C. Wang, "Modelling and control of nonlinear micro-distributed systems," to appear in *Proc. Second World Congress of Nonlinear Analyst*, Athans, Greece, 1996.

Appendix A

Consider the integral

$$\int_0^{2\pi}\int_0^1 K(\tilde{r},\theta,\rho,\xi)\tilde{\phi}_j(\rho,\xi)\rho d\rho d\xi = II(;) + I_2(\tilde{r},\theta) + I_3(\tilde{r}) + I_4(\tilde{r},\theta), \tag{A.1}$$

where

$$I_1(\tilde{r}) = \int_0^{271} d\xi(-\ln(\tilde{r}))\int_{J0}^{\tilde{r}} \tilde{\phi}_j(\rho,\xi)\rho d\rho, \tag{A.2}$$

$$I_2(\tilde{r},\theta) = -\int_0^{2\pi} d\xi \int_0^{\tilde{r}} \sum_{n=1}^{\infty} \frac{\rho^n}{n}(\tilde{r}^n - \tilde{r}^{-n})\cos(n(\xi-\theta))\tilde{\phi}_j(\rho,\theta)\rho d\rho, \tag{A.3}$$

$$I_3(\tilde{r}) = \int_0^{2\pi} d\xi \int_{\tilde{r}}^1 \ln(\rho)\tilde{\phi}_j(\rho,\xi)\rho d\rho, \tag{A.4}$$

$$I_4(\tilde{r},\theta) = -\int_0^{2\pi} d\xi \int_{\tilde{r}}^1 \sum_{n=1}^{\infty} \tilde{r}^n(\rho^n - \rho^{-n})\cos(n(\xi-\theta))\tilde{\phi}_j(\rho,\theta)\rho d\rho \tag{A.5}$$

The sum of the integrals I_1 and I_3 satisfies the estimate:

$$\begin{aligned} |I_1(\tilde{r}) + I_3(\tilde{r})| &\le \int_0^{2\pi} d\xi \left(-\ln(\tilde{r})\int_0^{\tilde{r}} \tilde{\phi}_j(\rho,\xi)\rho d\rho - \int_{\tilde{r}}^1 \rho\ln(\rho)\tilde{\phi}_j(\rho,\xi)d\rho\right) \\ &\le \int_0^{2\pi} d\xi \left(-\frac{1}{2}\ln(\tilde{r})\tilde{r}^2 - \int_{\tilde{r}}^1 \rho\ln(\rho)d\rho\right) \\ &= \pi(1-\tilde{r}^2)/2 \le \pi/2 \text{ for all } \tilde{r}\in[0,\ 1]. \end{aligned} \tag{A.6}$$

The sum of the integrals I_2 and I_4 can be bounded by

$$\begin{aligned} |I_2(\tilde{r},\theta) + I_4(\tilde{r},\theta)| &\le \int_0^{2\pi} d\xi \left(-\sum_{n=1}^{\infty}\frac{\tilde{r}^n - \tilde{r}^{-n})}{n}\int_0^{\tilde{r}} \rho^{n+1}\tilde{\phi}_j(\rho,\xi)d\rho \right. \\ &\quad \left. - \sum_{n=1}^{\infty}\frac{\tilde{r}^n}{n}\int_{\tilde{r}}^1 (\rho^{n+1} - \rho^{-n+1})\tilde{\phi}_j(\rho,\xi)d\rho\right) \\ &\le 2\pi\left(\sum_{n=1}^{\infty}\sum_{n=1}^{\infty}\frac{(\tilde{r}^2 - \tilde{r}^n)}{n(n+2)} + \tilde{r}(1-\tilde{r}) - \frac{1}{2}\tilde{r}^2\ln(\tilde{r}) + \sum_{n=3}^{\infty}\frac{(\tilde{r}^n - \tilde{r}^2)}{n(2-n)}\right) \\ &= 2\pi\left(\frac{2}{3}(\tilde{r}-\tilde{r}^2) - \frac{1}{2}\tilde{r}^2\ln(\tilde{r}) + 2\sum_{n=3}^{\infty}\frac{(\tilde{r}^2 - \tilde{r}^n)}{(n^2-4)}\right) \\ &\le 2\pi\left(\frac{2}{3} + g_1(\tilde{r}) + g_2(\tilde{r})\right) \quad \text{for all}(\tilde{r},\theta)\in\tilde{\Omega}_C, \end{aligned} \tag{A.7}$$

where

$$g_1(\tilde{r}) = -\tilde{r}^2\left(\frac{2}{3} + \ln(\tilde{r})\right), \qquad g_2(\tilde{r}) = 2\sum_{n=3}^{\infty}\frac{(\tilde{r}^2 - \tilde{r}^n)}{(n^2-4)}. \tag{A.8}$$

Using (A.7) and the fact that

$$\max_{0\le\tilde{r}\le 1} g_1(\tilde{r}) = g_1(\exp(-7/6)) = \frac{1}{2}\exp(-7/3),$$

$$\max_{0\le\tilde{r}\le 1}(\tilde{r}^2 - \text{in}) = \left(\frac{2}{n}\right)^{2/(n-2)}\left(\frac{n-}{n}\right. 2, \tag{A.9}$$

We have

$$\text{I'2(F!0,+'4(F,U)IS2T('3} \quad \frac{1}{2}\exp(-7/3)+ \sum_{n=3}^{\infty}\frac{2}{n(n+2)}\left(\frac{2}{n}\right)^{2/(n-2)}\Big) \text{ for all } (\tilde{r},\theta)\in\tilde{\Omega}_C. \tag{A.10}$$

Since $(2/n)^{2/(n-2)} < 1$ for all $n \geq 3$, thus

$$\sum_{n=3}^{\infty}\frac{2}{n(n+2)}\left(\frac{2}{n}\right)^{2/(n-2)} < \sum_{n=3}^{\infty} 2\mu(n), \tag{A.11}$$

where p(n) $= 1/(n(n+2))$. Using the fact that

$$\sum_{n=3}^{\infty} 2\text{P(n)} \leq \lim_{n\to\infty} 2\mu(n) + 2P(3) + \int_3^{\infty} 2\mu(x)dx = \frac{2}{15} - \ln(3/5), \tag{A.12}$$

we obtain the following estimate

$$|\, I_2(\tilde{r},\theta) \text{ i } I_4(\tilde{r},\theta)\,| \leq \pi\left(\frac{24}{15} + \exp(-7/3) - 2\ln(3/5)\right) \quad \text{for all } (\tilde{r}, \text{f?})\in\tilde{\Omega}_C \tag{A.13}$$

Combining (A.6) and (A.13) leads directly to the desired estimate (34)

Appendix B

For a center pad with normalized radius $\tilde{r}_1$, we partition the normalized mirror domain Ω_c into two disjoint subsets $\tilde{\Omega}_{p1} = \{(\tilde{r},\theta) : 0 \leq \tilde{r} < \tilde{r}_1, 0 \leq \theta \leq 2\pi\}$ and $\tilde{\Omega}_{p2} = \{(\tilde{r},\theta) : \tilde{r}_1 \leq \tilde{r} < 1, 0 \leq \theta \leq 2\pi\}$.

For $(\tilde{r},\theta) \in \tilde{\Omega}_{p1}$:

$$p(\tilde{r},\theta,u(\tilde{\text{x}}_j)) = \frac{q(u(\tilde{\text{x}}_j))r_o^2}{2T}\left(-\tilde{r}_1^2\ln\tilde{r}_1 + \frac{1}{2}(\tilde{r}_1^2 - \tilde{r}^2)\right); \tag{B.1}$$

and for $(\tilde{r}, \text{O}) \in \tilde{\Omega}_{p2}$:

$$p(\tilde{r},\theta,u(\tilde{\text{x}}_j)) = -\frac{q(u(\tilde{\text{x}}_j))}{2T}\tilde{r}_1^2\ln\tilde{r}, \tag{B.2}$$

where $u(\tilde{\text{x}}_j)$ corresponds to the mirror displacement at the circle with radius $\tilde{r} = \tilde{r}_1/2$, and

$$q(u(\tilde{\text{x}}_j)) = \frac{\epsilon_o}{2(d_o - u(\tilde{\text{x}}_j))^2}. \tag{B.3}$$

For a fan-shaped actuator electrodes with normalized spatial domain $\tilde{\Omega}_j = \{(\tilde{r},\theta) : \tilde{r}_j - \Delta\tilde{r}_j/2 < \tilde{r} < \tilde{r}_j + \Delta\tilde{r}_j/2, \theta_j - \Delta\theta_j/2 < \theta < \theta_j + \Delta\theta_j/2\}$, we partition the normalized mirror domain into four disjoint subsets $\tilde{\Omega}_{fi}, i = 1,\ldots,4$, defined by

$$\tilde{\Omega}_{f1} = \{(\tilde{r},\theta) : 0 \leq \tilde{r} \leq \tilde{r}_j^-, 0 \leq \theta \leq 2\pi\}; \qquad \tilde{\Omega}_{f2} = \tilde{\Omega}_j;$$

$$\tilde{\Omega}_{f3} = \{(\tilde{r},\theta) : \tilde{r}_j^+ < 1, 0 \leq \theta \leq 2\pi\};$$

$$\tilde{\Omega}_{f4} = \{(\tilde{r},theta) : \tilde{r}_j^- < \tilde{r} < \tilde{r}_j^+, \tilde{\theta}_j^- \geq \theta \geq \theta_j^+\}. \tag{B.4}$$

where $\tilde{r}_j^+ = \tilde{r}_j + \Delta\tilde{r}_j/2$, $\tilde{r}_j^- = \tilde{r}_j - \Delta\tilde{r}_j/2$, $\theta_j^- = \theta_j - \Delta\theta_j/2$, $\theta_j^+ = \theta_j + \Delta\theta_j/2$; and where $\Delta\tilde{r}_j$ and $\Delta\theta_j$ are the normalized radial width and the angular aperture of the fan-shaped actuator electrode respectively.

For $(\tilde{r}, \theta) \in \tilde{\Omega}_{f1}$:

$$p(\tilde{r},\theta,u(\tilde{\mathbf{x}}_j)) = \frac{q(u(\tilde{\mathbf{x}}_j))r_o}{2\pi T'}\Big\{\frac{\Delta\theta_j}{2}(\tilde{r}_j\Delta\tilde{r}_j - (\tilde{r}_j^+)^2\ln(\tilde{r}_j^+) + (\tilde{r}_j^-)^2\ln(\tilde{r}_j^-))$$

$$-\sum_{k=1}^{\infty}\frac{\tilde{r}^k}{k^2(k+2)}((\tilde{r}_j^+)^{k+2} - (\tilde{r}_j^-)^{k+2})[\sin(k(\theta_j^+ - \theta)) - \sin(k(\theta_j^- - \theta))]$$

$$+\sum_{k=1,k\neq 2}^{m}\frac{\tilde{r}^k}{k^2(2-k)}((\tilde{r}_j^+)^{2-k} - (\tilde{r}_j^-)^{2-k})[\sin(k(\theta_j^+ - \theta)) - \sin(k(\theta_j^- - \theta))]$$

$$+\frac{\tilde{r}^2}{4}\ln(\tilde{r}_j^+/\tilde{r}_j^-)[\sin(2(\theta_j^+ - \theta)) - \sin(2(\theta_j^- - \theta))]\Big\}; \qquad (B.5)$$

for $(\tilde{r}, \theta) \in \tilde{\Omega}_{f2}$:

$$p(\tilde{r},\theta,u(\tilde{\mathbf{x}}_j)) = \frac{q(u(\tilde{\mathbf{x}}_j))r_o^2}{2\pi T'}\Big\{\frac{\Delta\theta_j}{2} - (\tilde{r}_j^+)^2\Big(\ln(\tilde{r}_j^+) - \frac{1}{2}\Big)$$

$$-\sum_{k=1}^{\infty}\frac{1}{k^2(k+2)}(\tilde{r}^k(\tilde{r}_j^+)^{k+2} - (\tilde{r}_j^-)^{k+2}) + \tilde{r}^{-k}((\tilde{r}_j^-)^{k+2} - \tilde{r}_j^{k+2})[\sin(k(\theta_j^+ - \theta)) - \sin(k(\theta_j^- - \theta))]$$

$$+\sum_{k=1,k\neq 2}^{\infty}\frac{1}{k^2(2-k)}((\tilde{r}_j^+)^{2-k} - \tilde{r}^{2-k})[\sin(k(\theta_j^+ - \theta)) - \sin(k(\theta_j^- - \theta))]$$

$$+\frac{\tilde{r}^2}{4}\ln(\tilde{r}_j^+/\tilde{r})[\sin(2(\theta_j^+ - \theta)) - \sin(2(\theta_j^- - \theta))]\Big\}; \qquad (B.6)$$

for $(\tilde{r}, \theta) \in \tilde{\Omega}_{f3}$:

$$p(\tilde{r},\theta,u(\tilde{\mathbf{x}}_j)) = \frac{q(u(\tilde{\mathbf{x}}_j))r_o^2}{2\pi T'}\Big\{-\Delta\theta_j\tilde{r}_j\Delta\tilde{r}_j\ln(\tilde{r})$$

$$-\sum_{k=1}^{\infty}\frac{1}{k^2(k+2)}(\tilde{r}^k - \tilde{r}^{-k})((\tilde{r}_j^+)^{k+2} - (\tilde{r}_j^-)^{k+2})[\sin(k(\theta_j^+ - \theta)) - \sin(k(\theta_j^- - \theta))]\Big\}; \qquad (B.7)$$

and for $(\tilde{r}, \theta) \in \tilde{\Omega}_{f4}$:

$$p(\tilde{r},\theta,u(\tilde{\mathbf{x}}_j)) = \frac{q(u(\tilde{\mathbf{x}}_j))r_o^2}{2\pi T'}\Big\{\frac{\Delta\theta_j}{2}\Big((\tilde{r}_j^-)^2\ln(\tilde{r}_j^-) - (\tilde{r}_j^+)^2(\tilde{r}_j^+) - \frac{1}{2}\Big) - \frac{\tilde{r}^2}{2}\Big)$$

$$-\sum_{k=1}^{\infty}\frac{1}{k^2(k+2)}[(\tilde{r}^{k+2} - (\tilde{r}_j^-)^{k+2}(\tilde{r}^k - \tilde{r}^{-k}) + \tilde{r}^k((\tilde{r}_j^+)^{k+2} - \tilde{r}^{k+2})]\sin(k(\theta_j^+ - \theta)) - \sin(k(\theta_j^- - \theta))]$$

$$+\sum_{k=1,k\neq 2}^{\infty}\frac{\tilde{r}^k}{k^2(2-k)}((\tilde{r}_j^+)^{2-k} - \tilde{r}^{2-k})[\sin(k(\theta_j^+ - \theta)) - \sin(k(\theta_j^- - \theta))]$$

$$+\frac{1}{4}\tilde{r}^k\ln(\tilde{r}_j^+/\tilde{r})[\sin(2(\theta_j^+ - \theta)) - \sin(2(\theta_j^- - \theta))]\Big\}. \qquad (B.8)$$

FIGURE CAPTIONS:

Fig.1 Sketch of a circular micromachined deformable mirror in the form of a thin elastic surface with electrostatic actuators.

Fig.2 Typical actuator patches for rectangular and circular mirrors.

Fig.3 Graphs of $\mathcal{N}_{V_1^2}$ for the single actuator case with various values of κV_1^2

Fig.4 Srrm of the characteristic functions of the actuator spatial domains for a mirror with a center pad aud eight fan-shaped actuator electrodes $(\Delta x = \Delta y = r_o/30)$.

Fig.5 Actuator voltage pattern corresponding to V = (5, 10,5,35,10, 10,5,35, 10)^T volts $(\Delta x = \Delta y = r_o/30)$.

Fig.6 Norm of the difference of the mirror deformation u between two successive iterations as a function of iteration number.

Fig.7 (a) Computed mirror deformation; (b) radial profiles at O = 7r/4 (solid curve) aud $\pi/2$ radians (dashed curve); (c) level contours of the computed mirror deformation.

Fig.8 Norm of the difference of the mirror deformation **u** between two successive iterations as a function of iteration number starting with the flat mirror as the initial guess; $d_o = 6$ microns.

Fig.9 Level contours and surface of the desired mirror deformation given by Eq. (43) $(\Delta x = \Delta y = r_o/30)$.

Fig.1 O (a) Computed aud desired mirror deformations along a radial line at an angle of $\pi/4$ radians corresponding to **V** = (9.6254,30.1328, 41.7857,30 .1328,41.7857,30.1328,41.7857, 30.1328,41.7857)^T volts; (b) Difference between the desired and computed mirror deformations along a radial line at an angle of $\pi/4$ radians shown in (a).

Fig.11 Level contours and surface of the computed mirror deformation corresponding to **V given** in Fig.10(a).

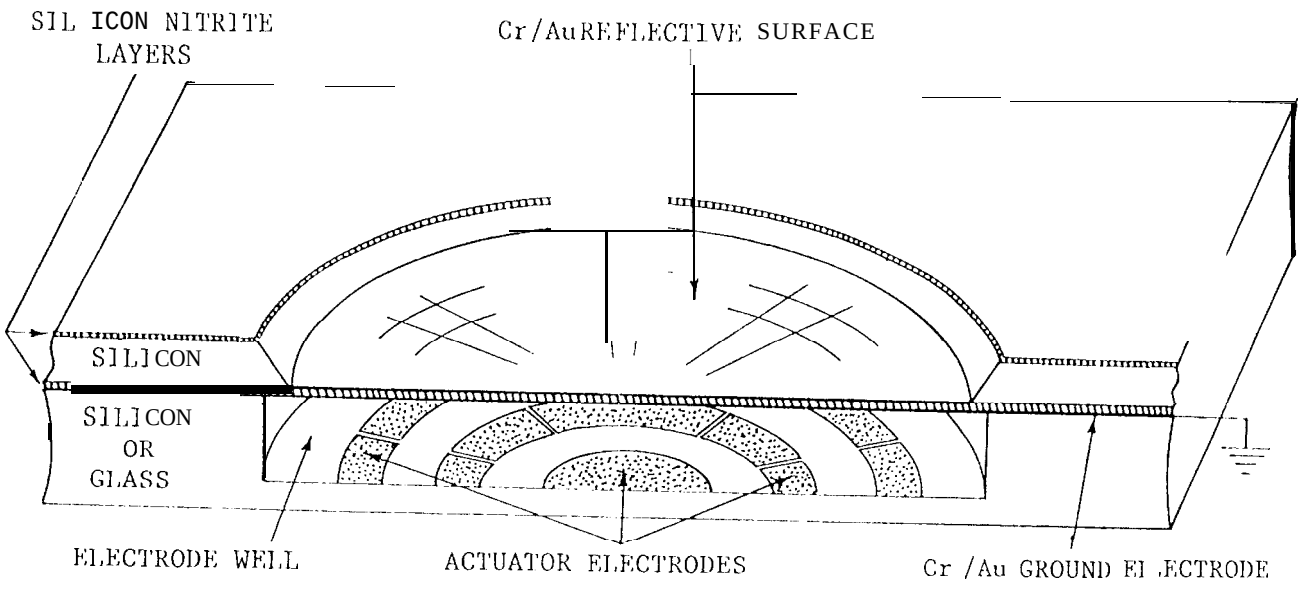
SIL ICON NITRITE
LAYERS
Cr/AuREFLECTIVE SURFACE
SILICON
SILICON
OR
GLASS
ELECTRODE WELL
ACTUATOR ELECTRODES
Cr /Au GROUND ELECTRODE

Fig. 1

RECTANGULAR MIRROR: $\Omega_R \triangleq \{(X_1, X_2) \in R^2: \; x_1 I \quad \ell_1, \; |x_2| < \ell_2\}$

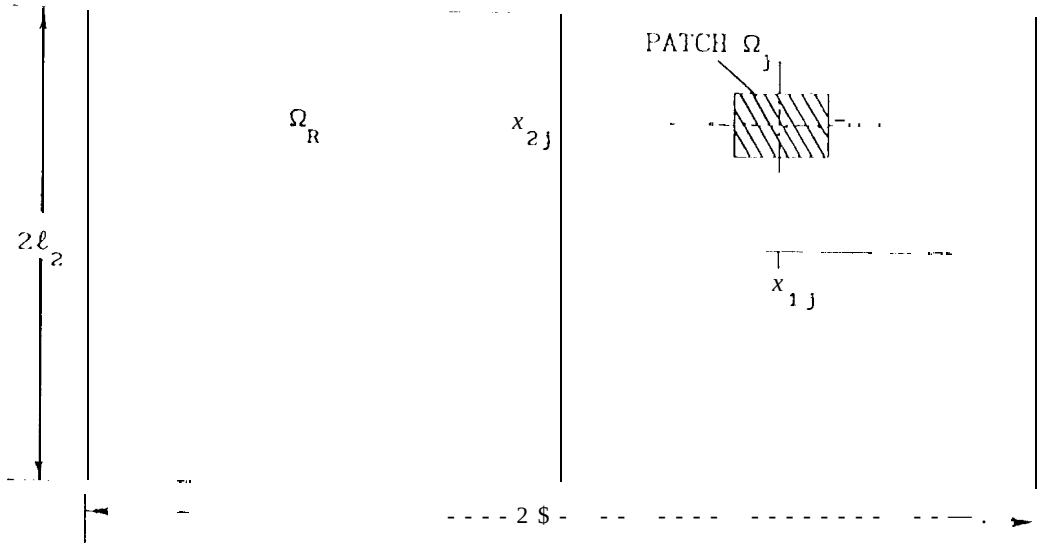

CIRCULAR MIRROR: $\Omega_C \triangleq \{(r, \theta): 0 \leq r < r_0, \; 0 \leq \theta \leq 2\pi\}$.

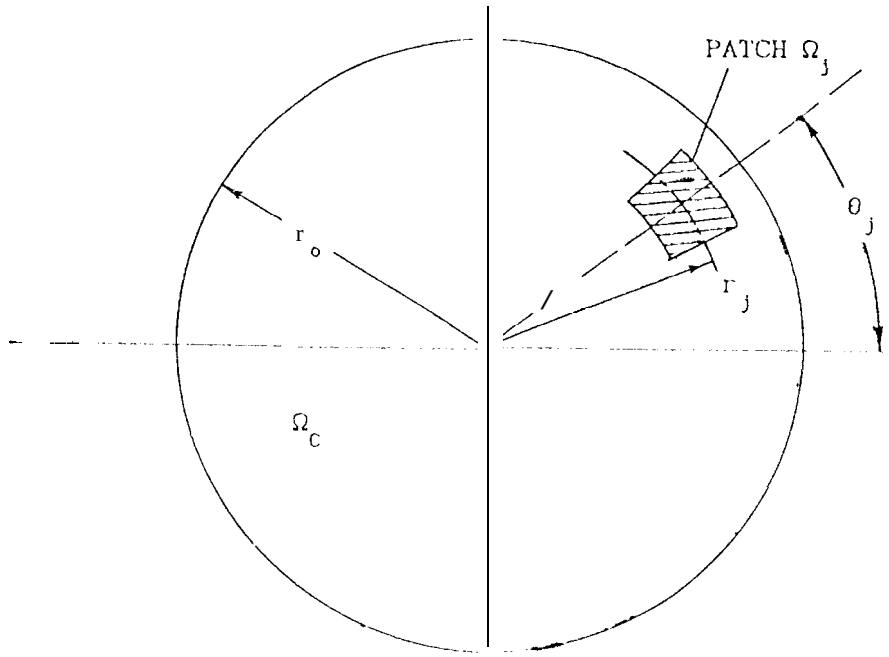

Fig. 2

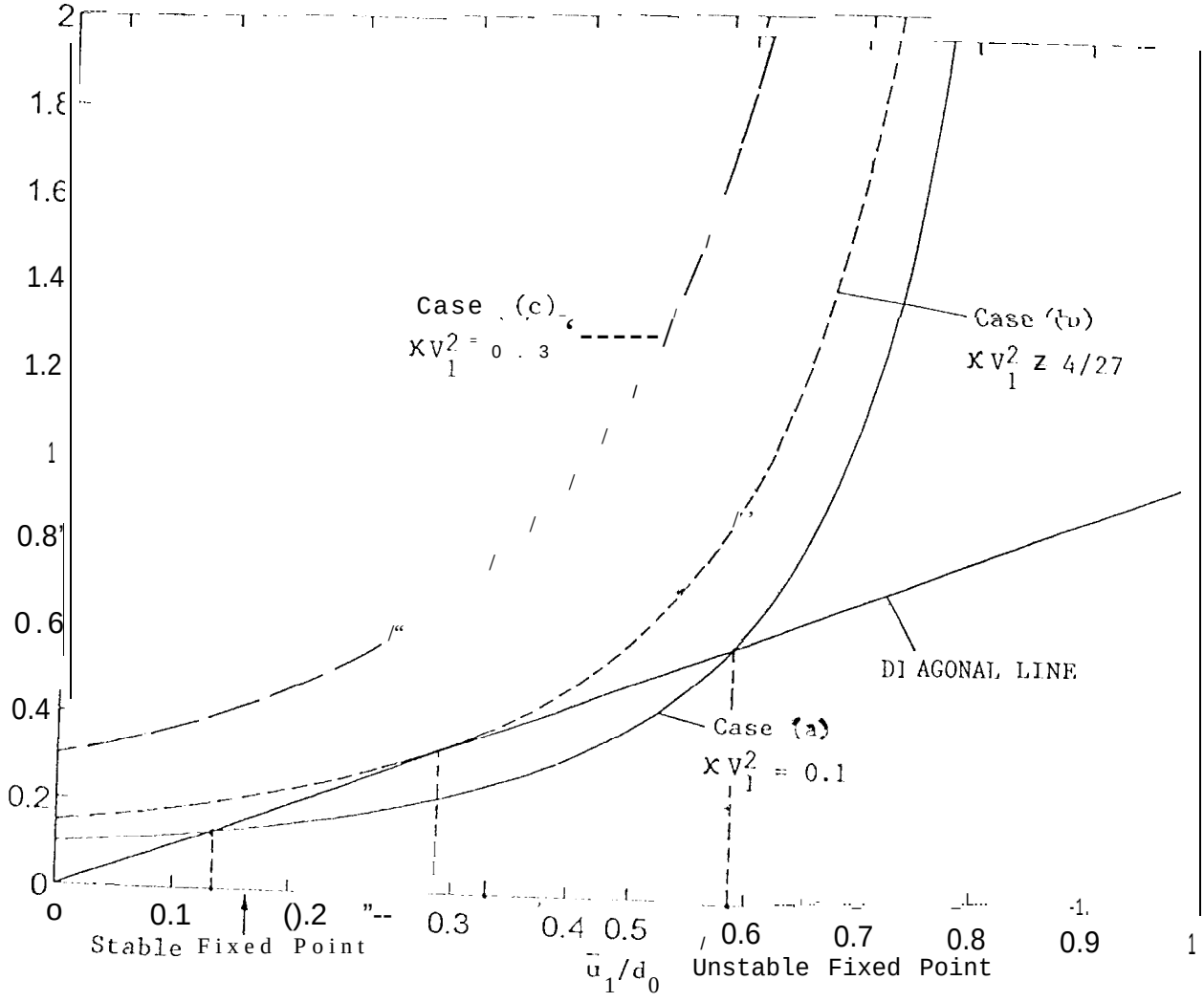
2
1.8
1.6
1.4
1.2
1
0.8
0.6
0.4
0.2
0
0
0.1
0.2
0.3
0.4
0.5
0.6
0.7
0.8
0.9
1
Case (c)
$\chi V_1^2 = 0.3$
Case (b)
$\chi V_1^2 = 4/27$
DIAGONAL LINE
Case (a)
$\chi V_1^2 = 0.1$
Stable Fixed Point
Unstable Fixed Point
u_1/d_0

Fig.3

ACTUATOR CONFIGURATION

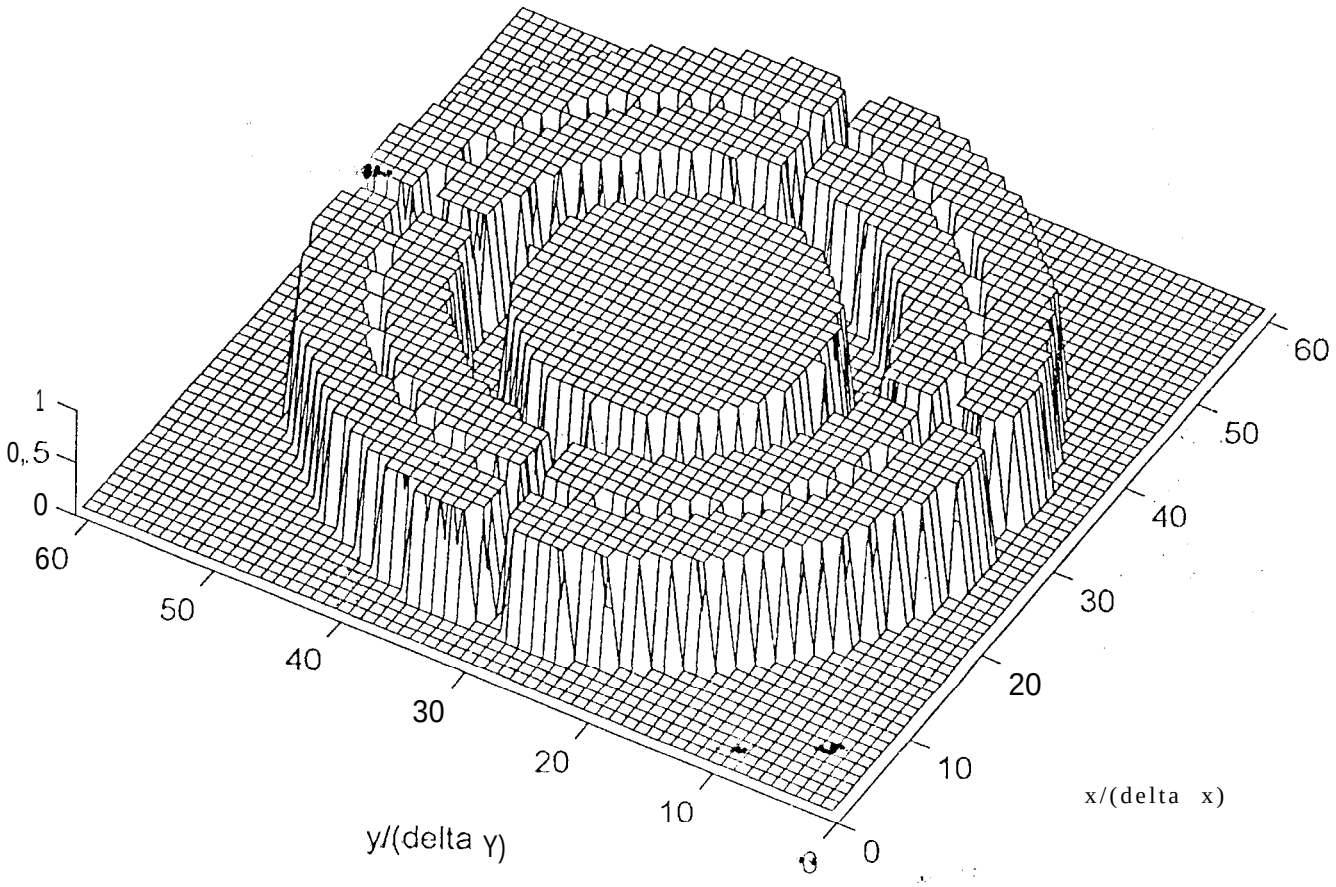

Fig. 4

ACTUATOR VOLTAGES

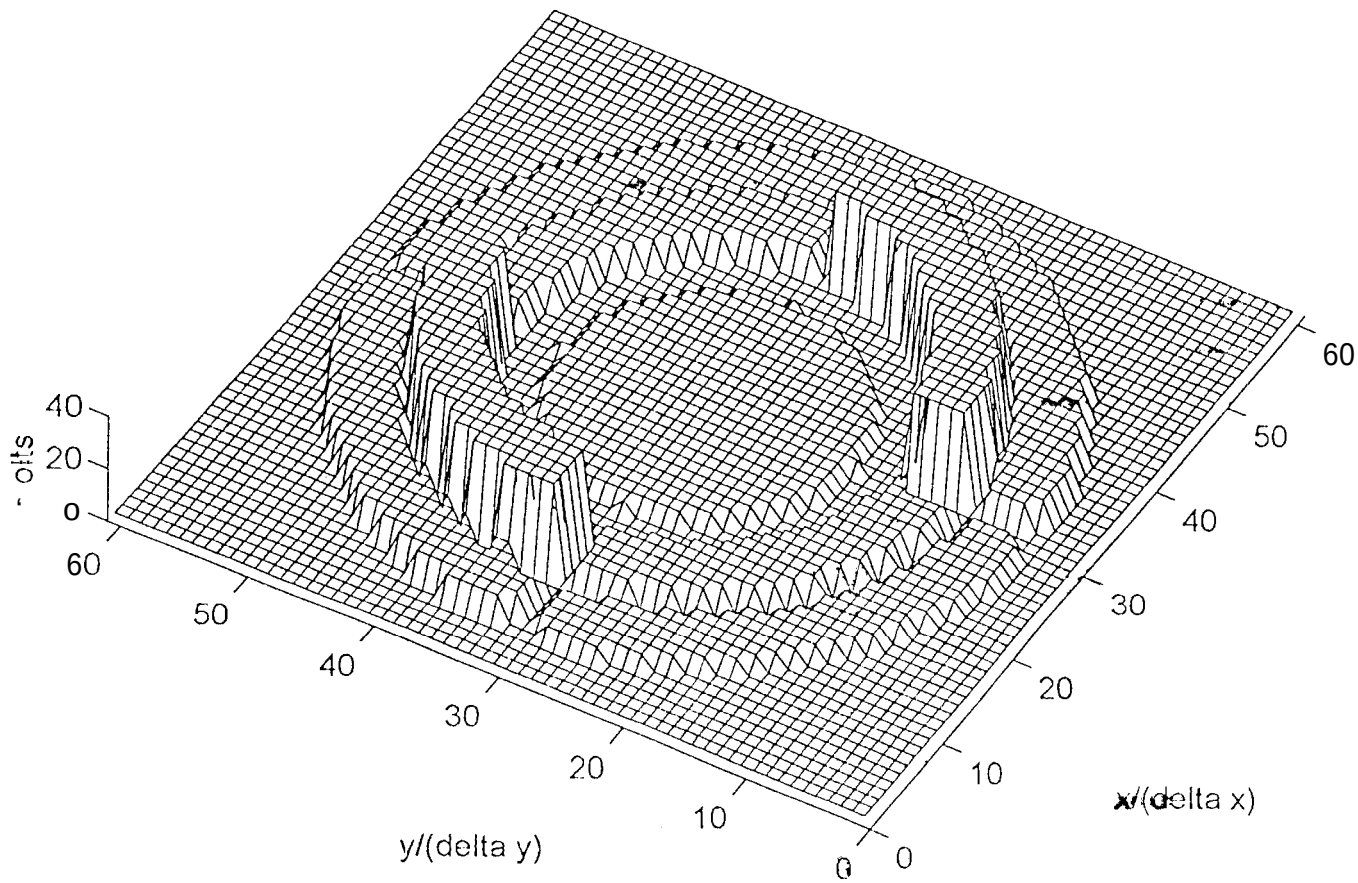

Fig.5

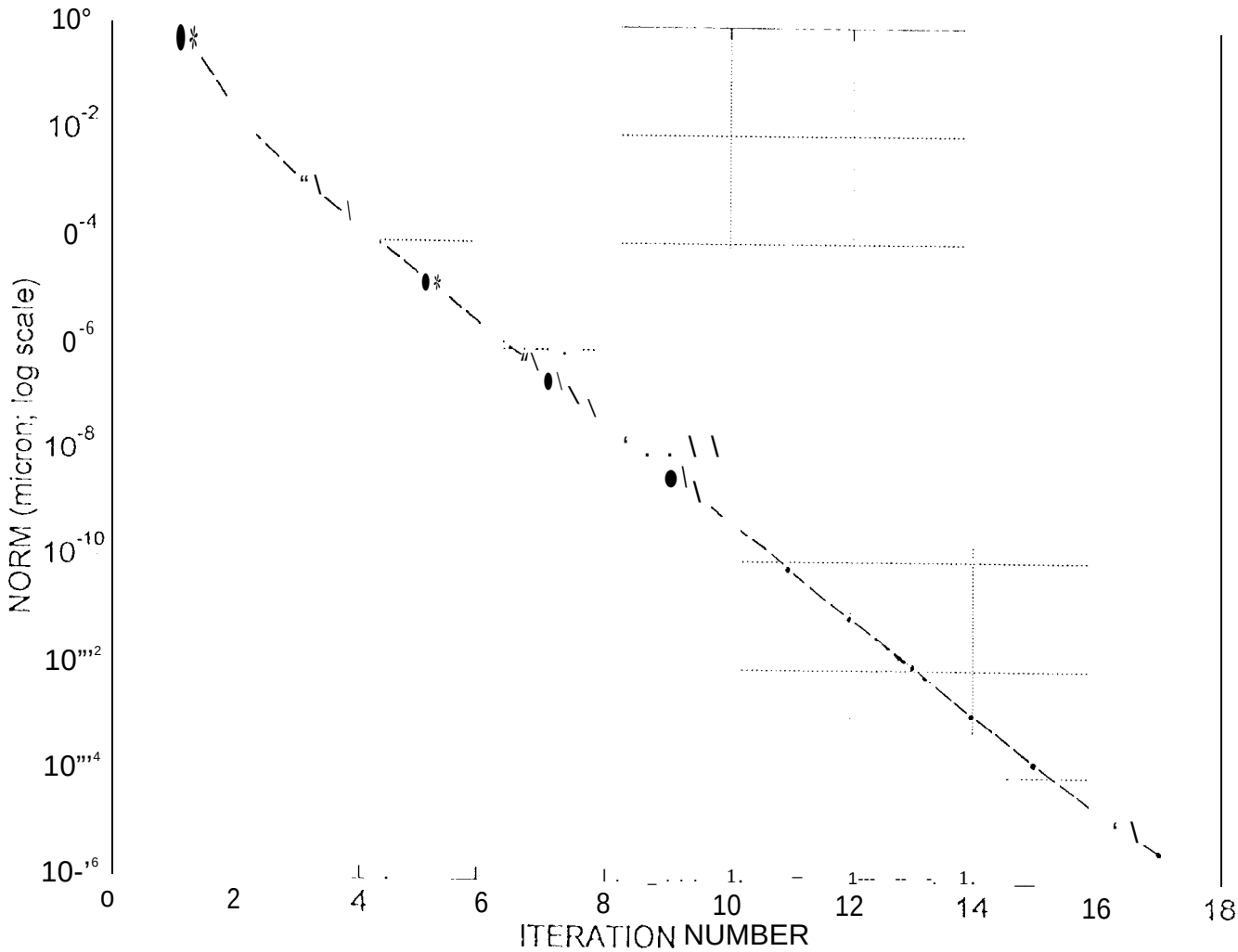
10°
10-2
0-4
0-6
10-8
10-10
10"'2
10"'4
10-'6
NORM (micron; log scale)
0
2
4
6
8
10
12
14
16
18
ITERATION NUMBER

Fig.6

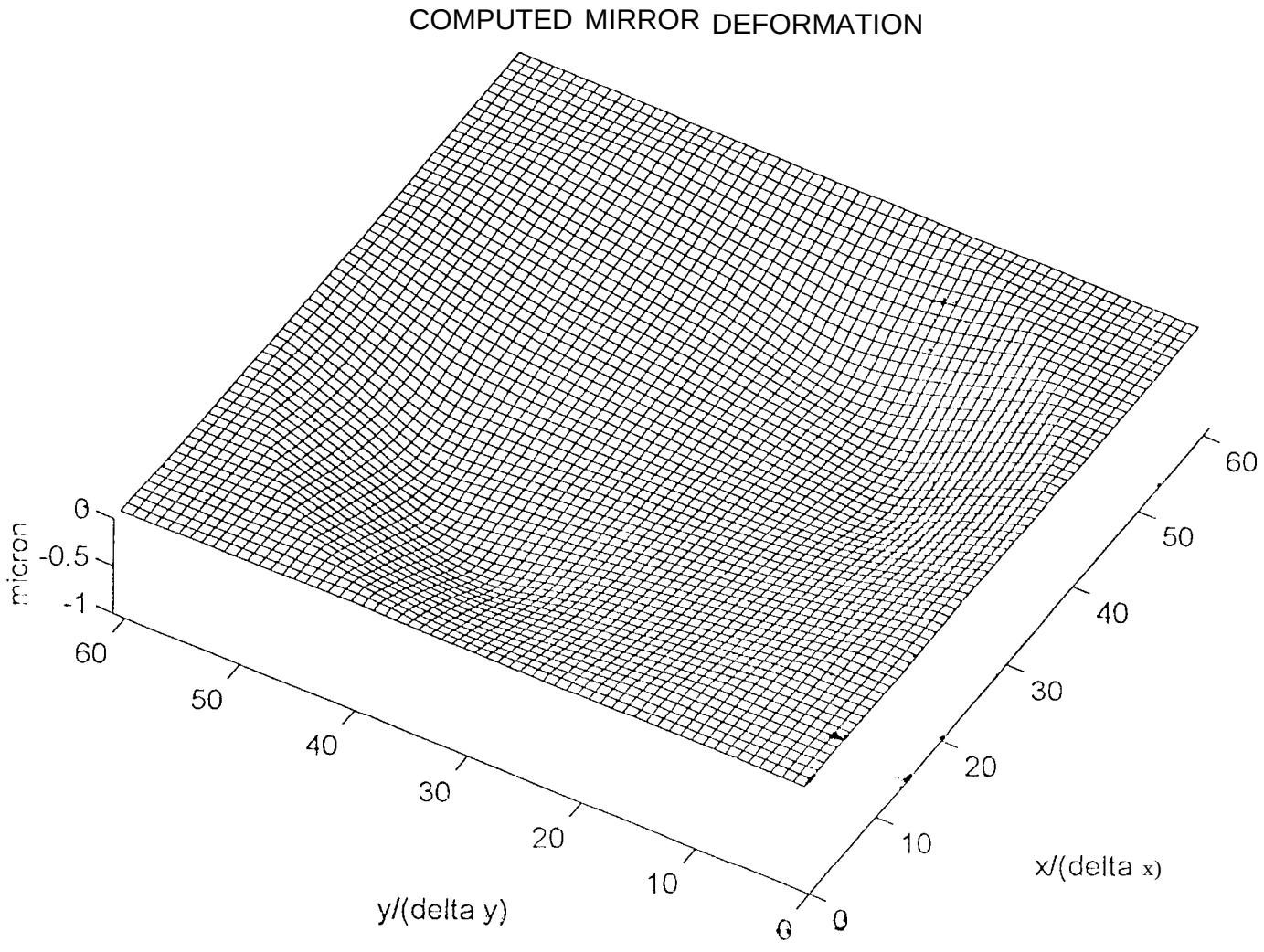
COMPUTED MIRROR DEFORMATION
micron
0
-0.5
-1
60
50
40
30
20
10
0
y/(delta y)
0
10
20
30
40
50
60
x/(delta x)

Fig.7a

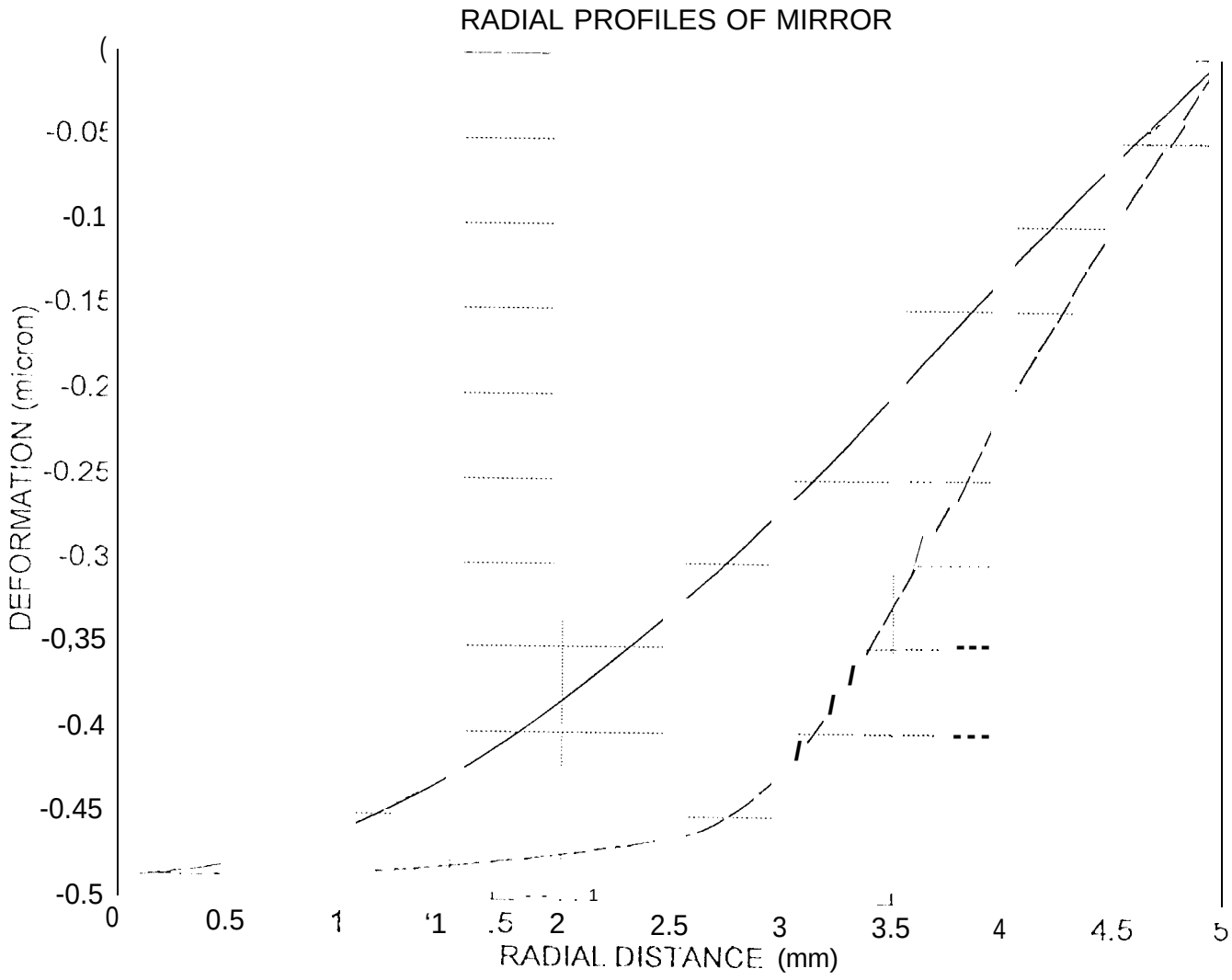
RADIAL PROFILES OF MIRROR
DEFORMATION (micron)
-0.05
-0.1
-0.15
-0.2
-0.25
-0.3
-0,35
-0.4
-0.45
-0.5
0
0.5
1
1.5
2
2.5
3
3.5
4
4.5
5
RADIAL DISTANCE (mm)

Fig. 7b

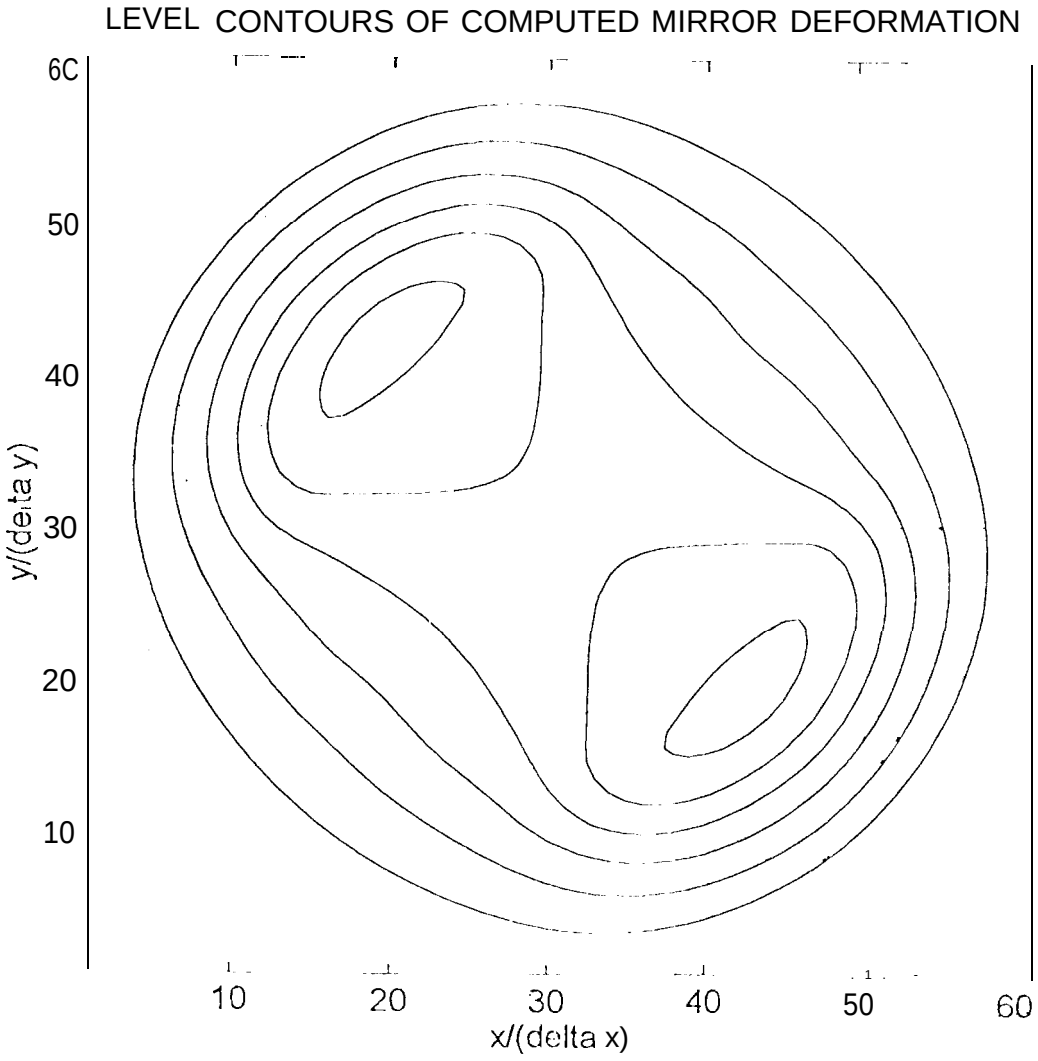
LEVEL CONTOURS OF COMPUTED MIRROR DEFORMATION
60
50
40
30
20
10
y/(delta y)
10
20
30
40
50
60
x/(delta x)

Fig.7c

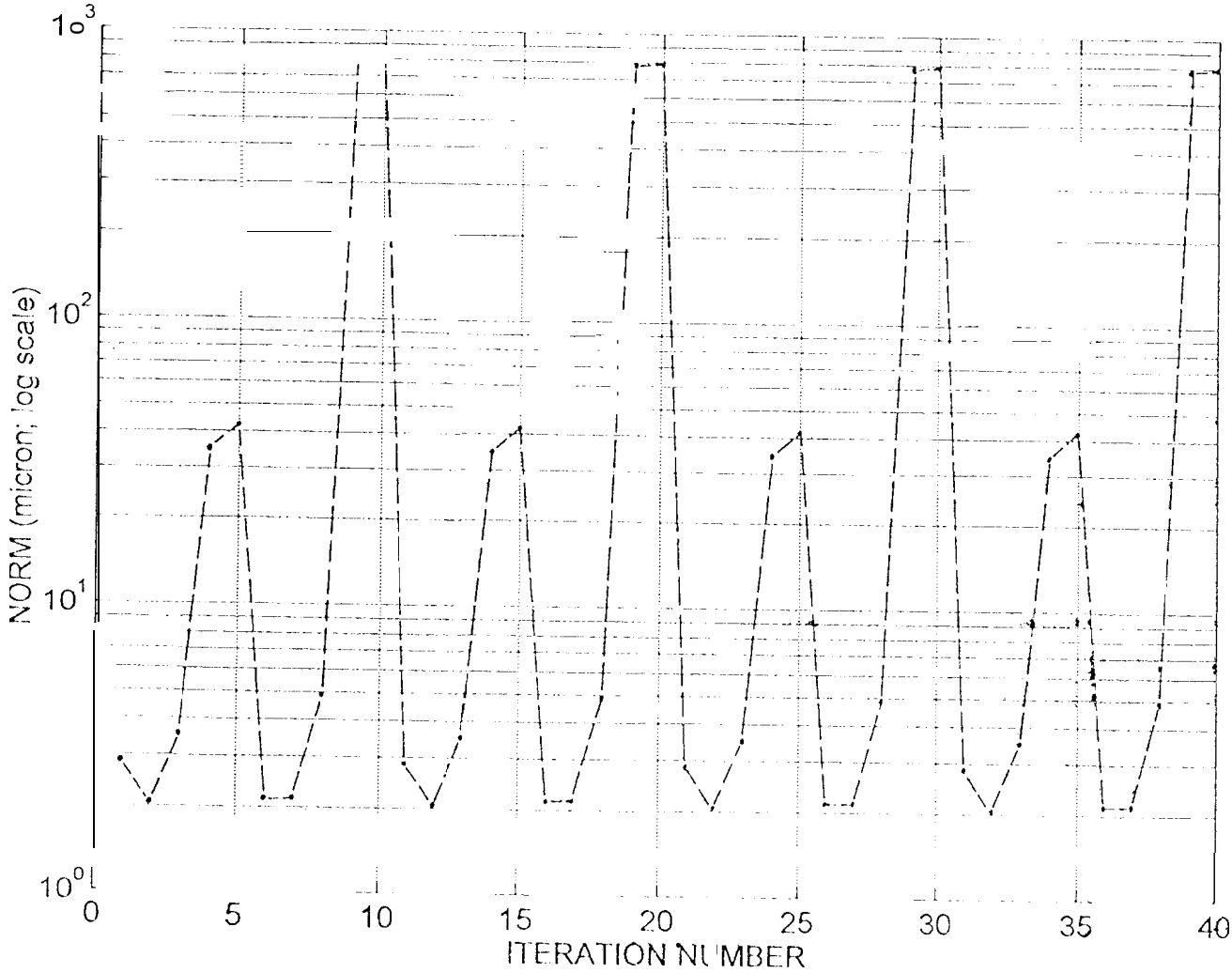
10^3
10^2
10^1
10^0
NORM (micron; log scale)
0
5
10
15
20
25
30
35
40
ITERATION NUMBER

Fig. 8

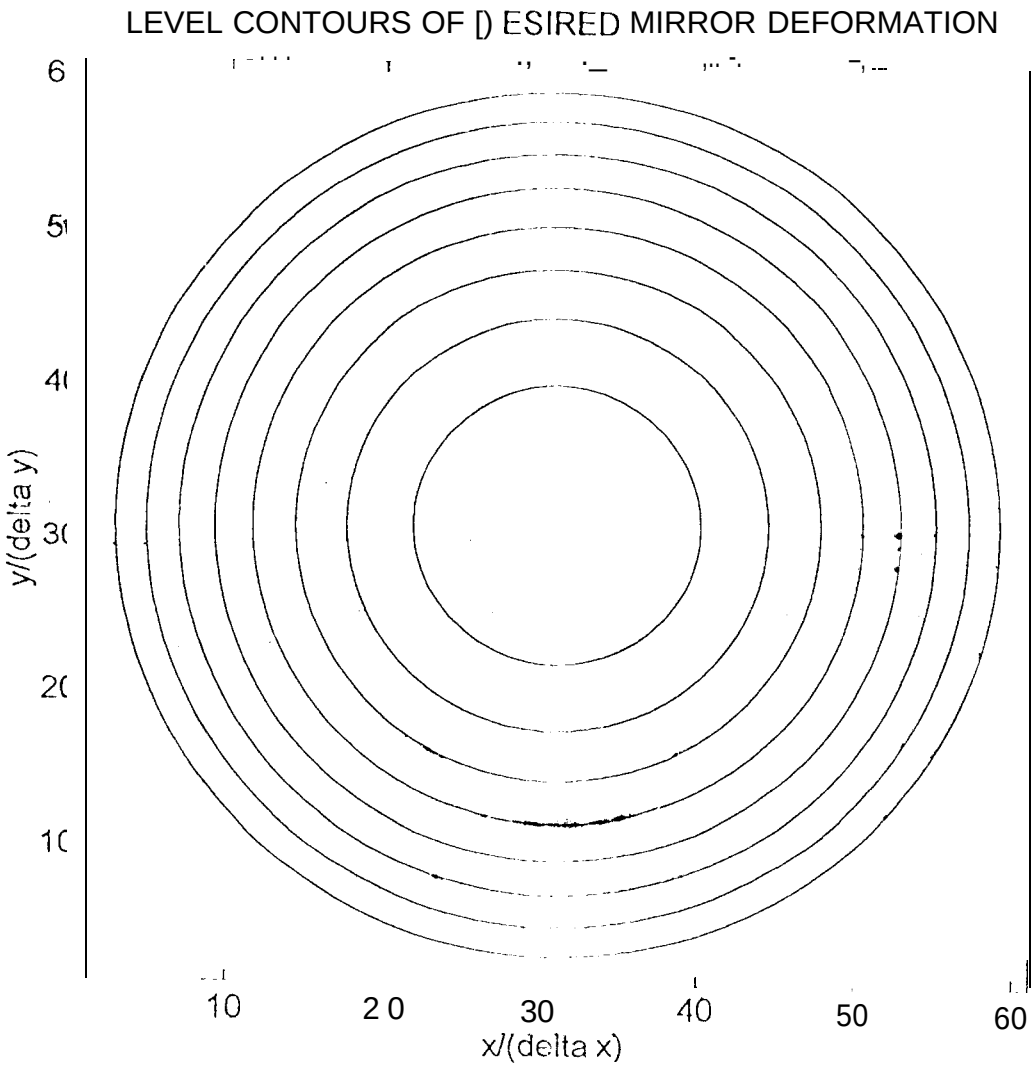
LEVEL CONTOURS OF [) ESIRED MIRROR DEFORMATION
6
5
4
3
2
1
y/(delta y)
10
20
30
40
50
60
x/(delta x)

Fig. 9a

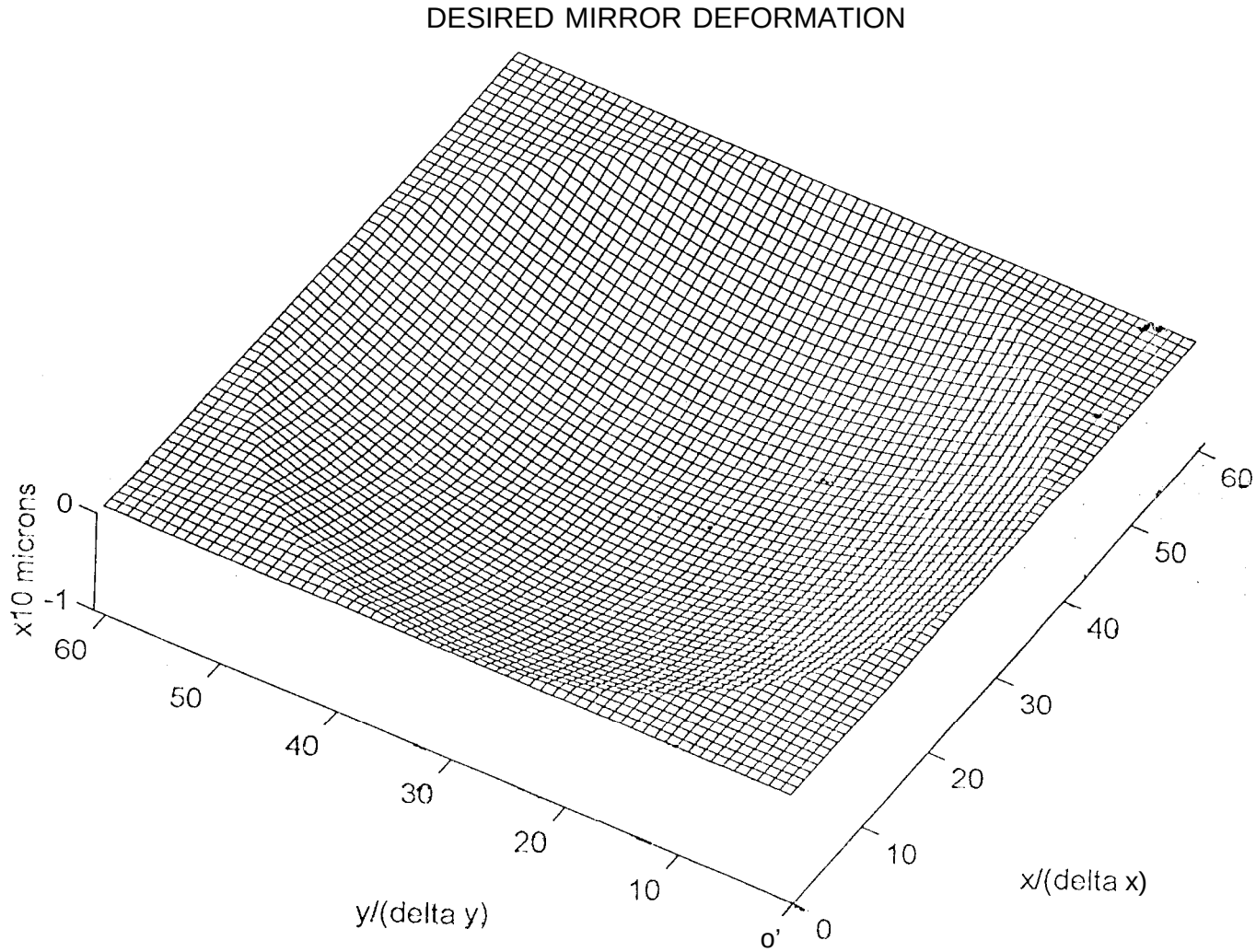
DESIRED MIRROR DEFORMATION
x10 microns
0
-1
60
50
40
30
20
10
y/(delta y)
o'
0
10
20
30
40
50
60
x/(delta x)

Fig.9b

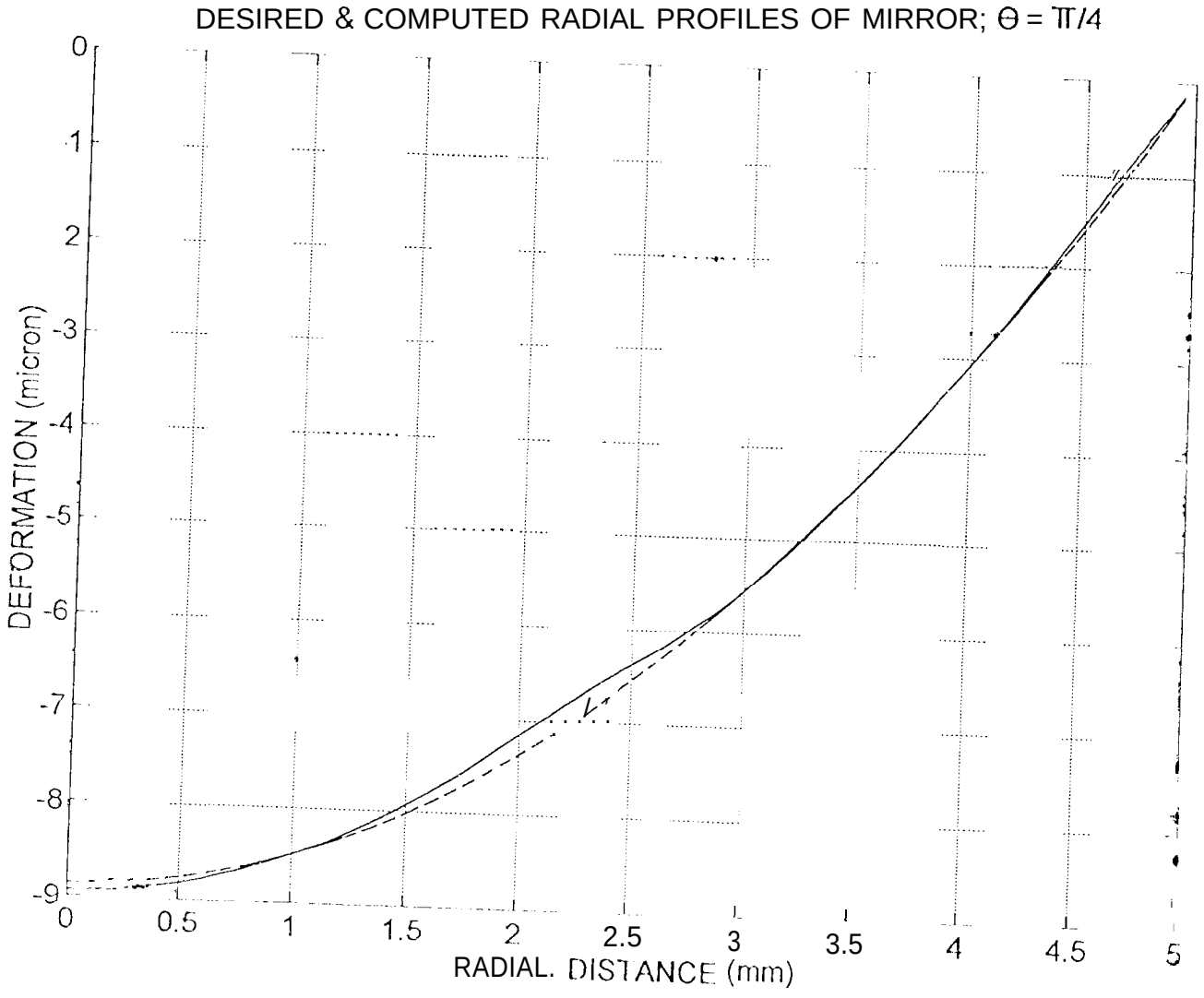
DESIRED & COMPUTED RADIAL PROFILES OF MIRROR; Θ = π/4
DEFORMATION (micron)
0
-1
-2
-3
-4
-5
-6
-7
-8
-9
0
0.5
1
1.5
2
2.5
3
3.5
4
4.5
5
RADIAL. DISTANCE (mm)

Fig. 10a

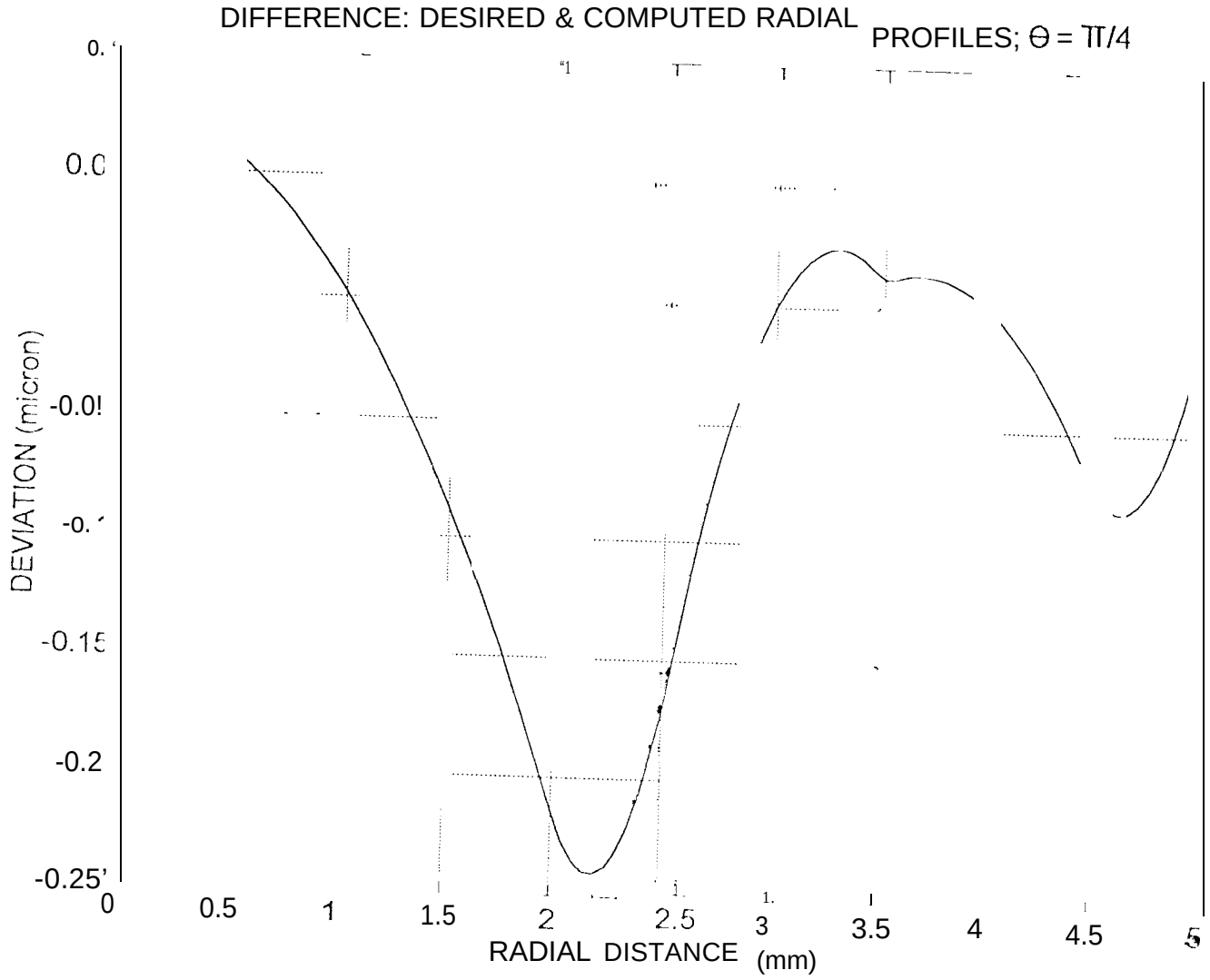
DIFFERENCE: DESIRED & COMPUTED RADIAL PROFILES; Θ = π/4
DEVIATION (micron)
0.0
-0.0!
-0.15
-0.2
-0.25
0
0.5
1
1.5
2
2.5
3
3.5
4
4.5
5
RADIAL DISTANCE (mm)

Fig.10b

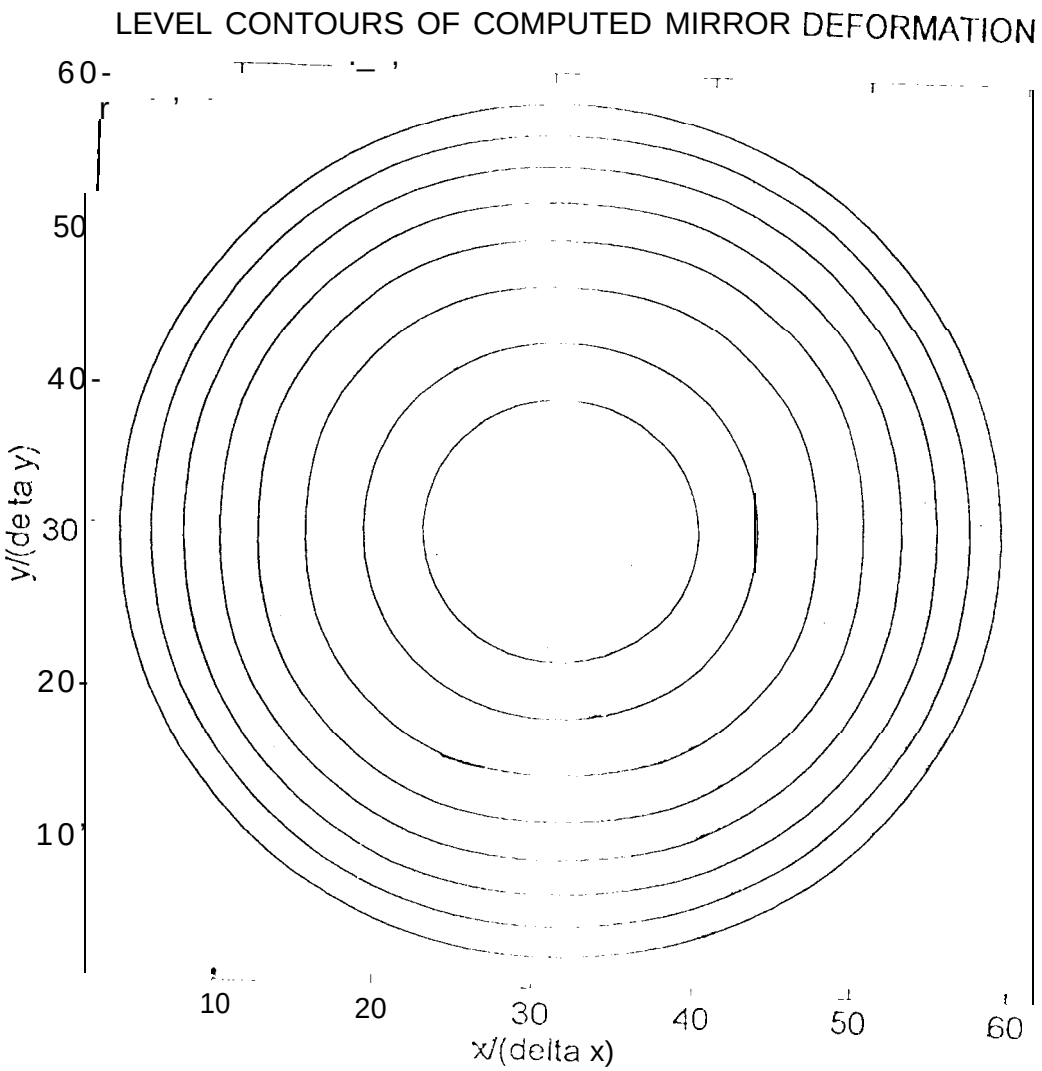
LEVEL CONTOURS OF COMPUTED MIRROR DEFORMATION
60
50
40
30
20
10
y/(delta y)
10
20
30
40
50
60
x/(delta x)

Fig. 11a

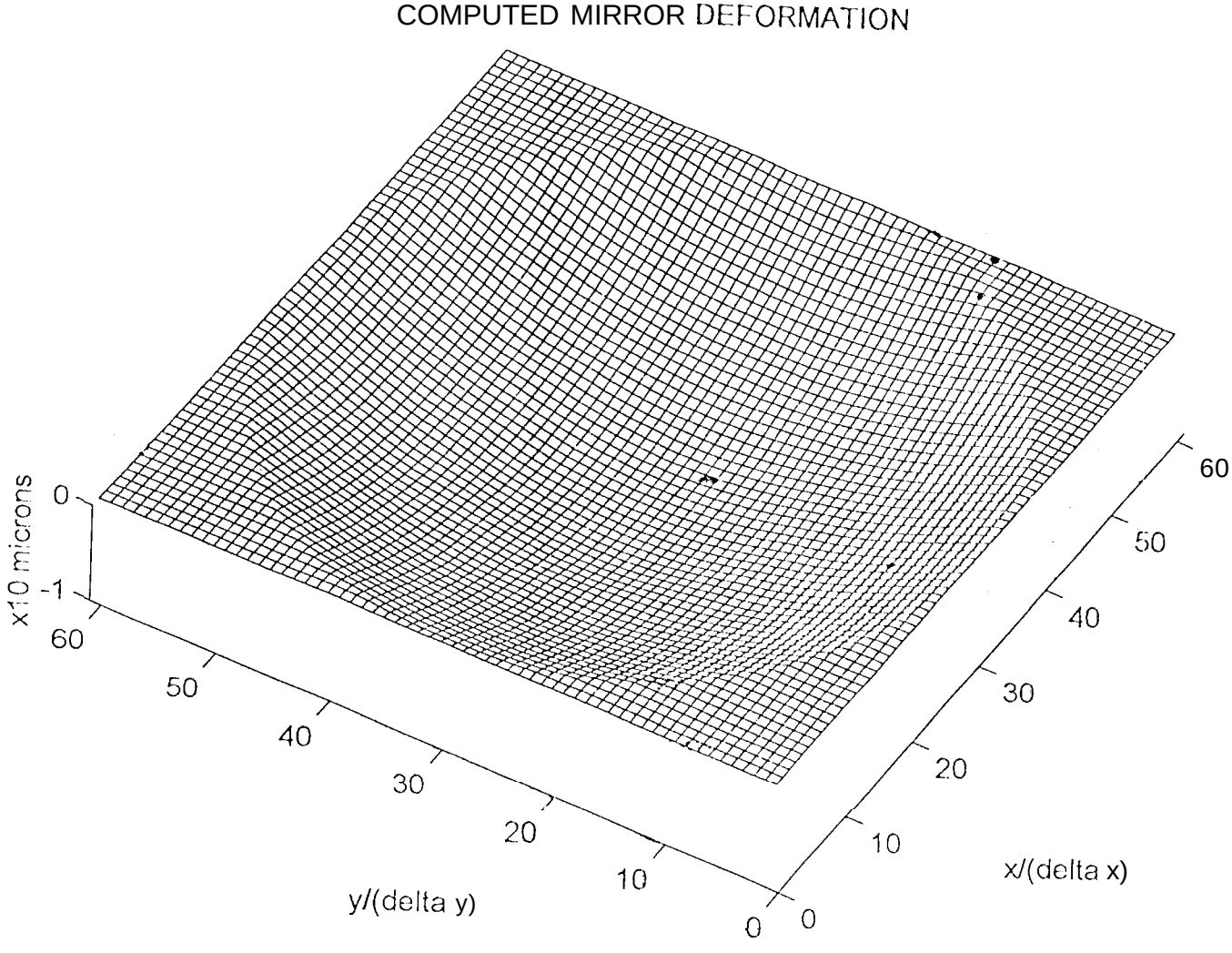
COMPUTED MIRROR DEFORMATION
x10 microns
0
-1
60
50
40
30
20
10
0
y/(delta y)
0
10
20
30
40
50
60
x/(delta x)

Fig. 11b